Estimating Sediment Yield from the Swift Creek Landslide, Whatcom County, Washington State

BY

CURTIS R. CLEMENT

Accepted in Partial Completion
of the Requirements for the Degree

Master of Science

Department of Geology
Western Washington University
Bellingham, Washington

Kathleen Kitto, Dean of Graduate School

ADVISORY COMMITTEE:

Dr. Robert Mitchell, Thesis Committee Chair

Dr. Doug Clark, Thesis Committee Advisor

Dr. Scott Linneman, Thesis Committee Advisor

MASTER'S THESIS

In presenting this thesis in partial fulfillment of the requirements for a master's degree at Western Washington University, I grant to Western Washington University the nonexclusive royalty-free right to archive, reproduce, distribute, and display the thesis in any and all forms, including electronic format, via any digital library mechanisms maintained by WWU.

I represent and warrant this is my original work, and does not infringe or violate any rights of others. I warrant that I have obtained written permissions from the owner of any third party copyrighted material included in these files.

I acknowledge that I retain ownership rights to the copyright of this work, including but not limited to the right to use all or part of this work in future works, such as articles or books.

Library users are granted permission for individual, research and non-commercial reproduction of this work for educational purposes only. Any further digital posting of this document requires specific permission from the author.

Any copying or publication of this thesis for commercial purposes, or for financial gain, is not allowed without my written permission.

Signature: _____

Date: _____

Estimating Sediment Yield from the Swift Creek Landslide, Whatcom County, Washington State

A Thesis
Presented to
The Faculty of
Western Washington University

In Partial Fulfillment
Of the Requirements for the Degree
Master of Science

by
Curtis R. Clement
July 2014

ABSTRACT

The amount of suspended sediment carried by streams in mountainous watersheds is an important factor in environmental and engineering planning, especially when the material happens to be of toxic nature. The Swift Creek watershed contains a deep-seated landslide composed of weathered serpentinite, which includes chrysotile (capable of asbestiform morphology), chlorite, illite, and hydrotalcite. The United States Environmental Protection Agency has determined that the asbestiform material contains particles of sufficient size and quantity that could be hazardous to human health. The suspended sediment load from Swift Creek is primarily influence by the steep, disturbed and unvegetated toe of the landslide which provides a large surface for overland flow directly into the stream creating temperamental conditions, as well as an effectively endless supply of sediment. The remainder of the watershed is heavily forested and consequently supplies relatively little sediment to the stream.

I attempted to develop a means to estimate sediment yield from the landslide, and provide a consistent method to monitor the stream in spite of the flashy conditions. I used the Distributed Hydrology-Soil-Vegetation Model to create a continuous discharge dataset from point discharge measurements. I also used the Turbidity Threshold Sampling method to collect physical water samples drawn during specific changes in turbidity and used the turbidity data as a proxy for suspended sediment. I developed linear models based on discharge and turbidity to estimate an annual yield.

Pacific Surveying and Engineering conducted a similar study three years after my data collection period and estimated a sediment yield that did not support my sediment yield estimates. The methods were slightly different as necessitated by the difference in quality of the various data types. As a result, I evaluated the differences between the methods in an effort to determine if the disparity between my estimate and Pacific Surveying and Engineering's estimate was caused by procedural differences. I included an analysis of timing between peak turbidity and precipitation and between peak turbidity and discharge. I found that the time between storms was important to the suspended sediment magnitudes. Future modeling efforts will need to incorporate this discharge-sediment hysteresis over the linear models in this research and by Pacific Surveying and Engineering.

The United States Geological Survey collected turbidity and discharge data on the Sumas River for several seasons. Monitoring here in the future will likely be more effective than monitoring Swift Creek directly because of the rivers discharge stability. If direct monitoring of the Swift Creek is to be continued, the relationship between discharge and suspended sediment should be further developed rather than turbidity and suspended sediment due to measurement stability.

ACKNOWLEDGEMENTS

I would like to thank my thesis committee for their guidance on the natural processes taking place at Swift Creek. Dr. Robert Mitchell provided substantial advice on scientific content and proper technical writing. I would like to thank Dr. Scott Linneman and Dr. Doug Clark for their time in the field, input and encouragement. Scott graciously spent time with me on the landslide and provided all the equipment that I used in the field.

I would like to thank Michael Hilles at the Institute for Watershed Studies for time spent training me to use their laboratory instruments and for advice in setting up my stream gauge. Paul Pittman provided invaluable data and spent personal time providing insight and encouragement. Dr. Chris Magirl of the USGS provided assistance and context in understanding turbidity data.

I would like to thank Tom Westergreen at Great Western Lumber for access to their roads along the Swift Creek. I would also like to thank the Western Washington University Geology Department for providing funding for this project.

TABLE OF CONTENTS

LIST OF TABLES

LIST OF FIGURES

1.0 INTRODUCTION

Swift Creek is a small stream the drains a large active landslide in northwest Washington, east of the cities of Everson and Nooksack (Figure 1). This landslide has been the subject of attention because of the abundant supply of suspended sediment and bedload it releases into the creek. The nature of the material and its influence on downstream ecosystems and human health has been the cause of added concern. The stream exhibits rapid changes in discharge, which makes data collection difficult but increased efforts have been made in the last decade to characterize the landslide material, its impact to the local and downstream societies through sediment transport and flooding, and the landslide mechanics.

The lower reaches of Swift Creek primarily pass through agricultural properties and clustered homes with several county maintained bridge crossings before flowing into the Sumas River where landslide derived sediments flow northward into SW British Columbia. The basin containing the landslide is mostly steep and forested on the flank of Sumas Mountain. A gentle alluvial fan extends into the bottom land below Sumas Mountain beginning just to the East of Goodwin Road Bridge and extends to the Sumas River. About 1.5 km of forested region along the river above Goodwin Road Bridge is maintained by Great Western Lumber Company (GWL) whose road provides the primary access to the landslide (Figure 1).

Although the slide has not exhibited catastrophic movement historically, it does release large quantities of sediment that ultimately affect the agricultural land and residential areas. The slide material and downstream deposits contain asbestos fibers from weathering of serpentinite involved in the landslide. Asbestos fibers are silicate mineral grains derived

from serpentine and amphibole minerals that can be toxic to humans when they are of sufficient length and width. In the case of Swift Creek, the fibers are being released from serpentinite contained in the landslide. Fibers that are longer than 5 mm and have a length to width ratio 3:1 are considered toxic (Department of Health, 2006). The sediments eroded from the Swift Creek landslide are designated as toxic because several samples that were collected in the field contained more than 1% asbestos (Swift Creek Sediment Management Action Plan, 2012).

For unknown reasons, the serpentinite is weathering unusually fast in the location of the landslide. The product of serpentinite weathering is a combination of asbestiform chrysotile, chlorite, illite, and hydrotalcite; chrysotile being the major constituent at up to 50% by volume (Bayer, 2006; Bayer and Linneman, 2010). The average size of chrysotile fibers is 2.0 μm in length. Length is a key dimension in asbestos toxicity to humans along with surface area, molecular structure, and adhesive properties (Holmes, 2012; Fubini and Arean, 1999; Gulumian, 2000; Oze and Solt, 2010).

The Washington State Department of Health (DOH) and the United States Environmental Protection Agency (EPA) performed research on the landslide material to evaluate the extent of the hazard to human health. The field-based studies of the EPA concluded that elevated cancer risks exist due to the concentration of asbestos fibers that are present (EPA, 2006 and 2011); however, the DOH findings indicated that asbestos related illness along the Swift Creek have occurred at lower rates than Whatcom County as a whole and of Washington State as a whole (DOH, 2010).

Now classified as hazardous waste and carrying potential health risks, Whatcom County must determine the most responsible and reasonable method to sequester and

dispose of the asbestos-baring material over the long-term. As such, knowledge of what factors affect the amount of sediment being eroded from the slide and an accurate quantification of the sediment discharge is crucial to develop cost effective and reliable remediation plans. Several agencies commissioned by Whatcom County have performed research on the Swift Creek watershed including Landau Associates, Kerr Wood Leidel Associates Ltd. (KWL), GeoEngineers, and Pacific Surveying & Engineering (PSE); additional studies were performed by Western Washington University, BGC Engineering, Washington State Department of Ecology (DOE), Washington State Department of Health (DOH), United States Environmental Protection Agency (EPA) and Bennett Engineering (Table 1). The PSE study investigated the annual sediment yield and the potential use of large holding pits as a collective sink for sediment (PSE, 2012). The methods employed were similar to the methods in my research and the results are compared in this document.

One of the major objectives of Swift Creek research is to determine an annual sediment yield. Previous studies have estimated the total annual sediment discharge to be between 68,810-91,750 m^3/yr (90,000 – 120,000 yds^3/yr) (McKenzie-Johnson, 2004); 86,390 m^3/yr (113,000 yds^3/yr) (PSE, 2012) and an annual suspended sediment yield of 4,616 m^3/yr (910 tons/km^2/yr, 6,038 yds^3/yr, Bayer, 2006). Suspended sediment loads have been estimated at ranges between 0.02 g/L to 41.6 g/L and discharge rates between 0.0 m^3/s to 0.5 m^3/s (Bayer, 2006; Bayer and Linneman, 2010). With the assumption that the majority of the sediment being transported by Swift Creek comes from the landslide toe, the erosion rate is estimated at ~1m/yr (Bayer and Linneman, 2010). In the lower energy state section of Swift Creek, before entering the Sumas River, approximately 30,580 m^3/yr (40,000 yd^3/yr) were deposited between 1999-2002 (KWL, 2005; DOH, 2006).

Sediment transported down Swift Creek and into Sumas River often fills channels that have to be dredged to prevent flooding and road damage. Flooding can leave significant amounts of asbestos laden material in public and private property where it can become airborne by various activities (DOH 2010, EPA 2006 & 2011). Dredging was initiated in the 1950s by the Army Corps of Engineers in order to mitigate flooding; dredging responsibilities were later assumed by Whatcom County Public Works (Swift Creek Sediment Management Action Plan (SCSMAP), 2012). In previous years the dredged material was piled next to the creek and used in a variety of ways, such as fill dirt in newly constructed residential areas and other construction sites. Dredging and the private use of the material served as a temporary flood control and waste disposal plan which eventually became financially prohibited due to regulations imposed because of potential health risks.

Numerical models are useful tools for examining hydrologic and mass wasting problems such as those in the Swift Creek basin. One example is the Distributed Hydrology-Soil-Vegetation Model (DHSVM) that was developed by the University of Washington (UW) and the Pacific Northwest National Lab (e.g., Wigmosta et al., 1994; Doten and Lettenmaier, 2004; Doten et al., 2006). The DHSVM is a spatially distributed, physically based hydrologic model that I used to estimate discharge for Swift Creek. An additional module to quantify sediment transport and predict slope stability exists and is primarily used to quantify sediment from logging roads and deforestation as a result of logging and fires. At Western Washington University, the DHSVM has been used to model river discharge for water budgets, forest cover effects on surface water and ground water, glacial recession, climate change effects and slope failure probabilities (e.g., Chennault, 2004; Kelleher, 2006; Donnell, 2007; Dickerson, 2010; Hanell, 2011; Brayfield, 2013).

The Swift Creek watershed and landslide material pose unique challenges to local, state, and federal agencies. The watershed contains a landslide with poor access and material that is considered hazardous to human health. The quantity of sediment and the timing of sediment delivery are poorly understood and require further study. My research provides an estimate of sediment yield during the winter season of 2008-09 and information about how precipitation rates influence stream discharge and erosion from the unvegetated landslide toe.

2.0 BACKGROUND

2.1 Swift Creek Watershed

2.1.2 Basin Characteristics

The Swift Creek basin consists of an upper and lower basin. The upper basin on Sumas Mountain contains the sub-basins of the North Fork and South Fork Swift Creek. The Swift Creek landslide resides in the South Fork sub-basin. My study incorporated parts of the upper and lower basins from the Goodwin Road Bridge, containing ~6.5 km^2 with nearly 1000 m of relief with elevations ranging from ~35 m to ~1040 m (Figure 1). The lower basin by itself is estimated to be 2 km^2 (SCSMAP, 2012). The estimated size of the upper and lower Swift Creek basin together is ~7.1 km^2 (Bayer and Linneman, 2010).

The primary forest cover on Sumas Mountain is coniferous, but some deciduous trees grow in pockets at lower elevations along stream gullies and landslide margins. Sumas Mountain is a local logging resource and several areas within the Swift Creek basin have been clear cut. Soil types range from silty loam to very gravelly loam (United States Department of Agriculture, Natural Resources Conservation, State Soil Geographic (STATSGO), 2001). Precipitation measured on the toe of the landslide is consistent with the western Cascade foothills in Washington, receiving in excess of 100 cm annually (Western Regional Climate Center, 2013).

Some geographic nomenclature has been established in the SCSMAP (2012). It should be noted that the boundary of the upper basin follows the hydrologic boundaries but the boundary of the lower basin, as defined in the SCSMAP, follows the mapped perimeter of the alluvial fan, which cuts across hydrologic boundaries. The North and South Forks converge near the fan apex (Figures 2 and 3).

As stated, the upper basin contains the landslide and headwaters of the north and south forks of Swift Creek. The lower watershed is divided into three reaches known as the Canyon Reach, Goodwin Reach and Oat Coles Reach. These are defined by streambed characteristics such as channel confinement, gradient and substrate. An additional tributary watershed containing the Great Western Creek is not defined in the SCSMAP but enters into the Swift Creek system along the Canyon Reach.

2.1.4 Stream Characteristics

Swift Creek has two forks: the North Fork, also known as Goldmine Creek flows through forest until it converges with the South Fork below the landslide (SCSMAP, 2012; Figure 2). The South Fork is 1.5 km long and is fed by two streams that drain the landslide flanks and unvegetated toe. From the toe, the stream has cut a narrow, steep sided channel through a conglomerate body. Further downstream, the channel opens up and is littered with boulders, cobbles and gravel from high water events. Eventually the Swift Creek enters farm land where it is controlled by dredge piles left along the stream bank before flowing into the Sumas River. This lowest section is characterized by the deposition of the fine asbestos contaminated sediments. The beginning of this section of the creek is at Goodwin Road Bridge, which is where the discharge and sediment concentration data were collected for this study.

The North and South Fork have similar elevation extents and average gradients on the order of 20%; however, the North Fork flows clear through heavy forest and supports an isolated wild trout population (SCSMAP, 2012). Both forks flow year round but the South Fork is the primary source of sediment downstream (Bayer and Linneman, 2010). At low flows in the summer, the South Fork and downstream reaches become clear with little

landslide-derived sediments; the streambed scours slightly during these times. Winter flows are moderate to flood level with high concentrations of suspended sediment during storm events. During the winter season there can be rapid channel infilling from high turbidity discharge while scouring occurs between storms. The sediment volumes deposited during infilling events exceeds scouring, resulting in an overall annual aggradation of the streambed.

The Canyon Reach begins at the top of the lower basin as the South Fork crosses onto the alluvial fan apex and includes the confluence of the North and South Fork as well as the Great Western Creek (SCSMAP, 2012; Figure 3). The Canyon Reach is aptly named due to the steep constrictive banks. The gradient in this reach diminishes from 8% at the top to 5% at the bottom. The streambed primarily contains cobbles and gravel with boulders. The Goodwin Reach begins at the point the stream exits the foothills and ends at the Goodwin Road Bridge (SCSMAP, 2012). The gradient begins to flatten from 5% at the top to 1% at the bottom, resulting in a decreased energy state and the deposition of smaller gravel, sand and silt. Cobbles are likely to be found in the upper portions of this reach.

The Oat Coles Reach begins at the Goodwin Road Bridge and extends to the Sumas River (SCSMAP, 2012). Oat Coles Road Bridge crosses Swift Creek ~500 m above the confluence with the Sumas River. In the reach the gradient varies between 1.3% and 0.2%. Sediment deposits at Oat Coles Road Bridge are predominantly sand.

2.1.1 Geology

The Swift Creek landslide (SCL) is about 55 hectares and lies on the steep western slope of Sumas Mountain. Dragovich et al. (1997) identified two major bedrock units near the slide: the Huntingdon conglomerate and an ultramafic body primarily composed of serpentinite. A small deposit of glacial till is mapped on the south side of the slide (Figure 4).

The serpentinite body appears to form the basal slide plane of the landslide and is considered to be the source of the asbestiform material that results from rapid weathering and disaggregation of chrysotile fibers (Bayer, 2006). In the area surrounding the toe of the slide, the Huntingdon conglomerate overlies the serpentinite (Dragovich et al., 1997). The conglomerate bordering the toe has been undercut in places and toppled leaving massive boulders on top of the landslide toe. The conglomerate also forms isolated constrictions along Swift Creek downstream from the toe of the landslide.

2.1.3 Landslide Mechanics and Mineralogy

McKenzie-Johnson (2004) classified the slide as a slow moving, deep-seated landslide. There are three basic zones defined by their characteristic morphology and motion: the zone of depletion, the neutral zone, and the zone of accumulation. The zone of depletion comprises the upper third of the slide where thinning is occurring and is manifested by a series of extensional head scarps. The neutral zone comprises the central third where the slide is moving mainly as a coherent block with little surface deformation; consequently, this zone is covered with a dense stand of large evergreen trees. The zone of accumulation includes the thick, over steepened, unvegetated toe. Small, shallow slope failures occasionally occur on the toe. These small surficial releases have been recorded by

time-lapse photography as part of the Western Washington Landscape Observatory (Linneman and Clark, 2006). In addition to mass wasting from the toe, abundant surface erosion results from rainfall on the unvegetated surface.

Slide velocity varies spatially. Maximum velocities occur at the toe and are as rapid as 30 m/yr (McKenzie-Johnson, 2004). Upper parts of the slide move about 4 m/yr. The greater velocities at the toe cause discontinuous expansion fractures to form at the top of the toe where the velocity gradient is greatest. The fractures are roughly parallel to surface contours indicating that surface flow is parallel to the slope. The fractures are typically centimeters in width and several meters in length and may form the head scarps to the small surface failures on the toe. Slide motion for the years between 2004 and 2008 has been estimated at 4-5 m/yr from GPS surveys (Linneman, 2009). An earlier estimate made by Converse et al. (1976) of slide movement did not differentiate the spatial variance but overall the velocity was estimated at 9 m/yr based on historic aerial photographs (SCSMAP, 2012).

A common term for prolonged motion of this magnitude for a landslide is ‘creep’ (Radbruch-Hall, 1978). The velocities noted above are annual averages and vary seasonally, probably due to changes in the water table and its effect on the effective normal stress between sediment grains (McKenzie-Johnson, 2004). Another possible cause for changes in the rates of landslide creep includes earthquakes, as observed at the Point Firmin landslide in California (Miller, 1931). Although seismic induced changes have not been documented at the SCL, it is a viable mechanism for future motion in this seismically active area.

Depth of the shear plane is estimated between 90 – 125 m (McKenzie-Johnson, 2004). This estimate was determined by projecting the head scarp trajectory to the toe using a high-resolution GPS-based topographic profile. At these depths, the stress-strain relationship and the mechanics of motion are not as well understood in comparison to shallow slides (Petley and Allison, 1997). McKenzie-Johnson (2004) made several alternative predictions of the depth and trajectory of the shear boundary based on different factor of safety values. The projected detachment trajectory combined with the slide area of about 550,000 m^2, indicates the landslide volume is between 3.5 x 10^7 m^3 to 5.1 x 10^7 m^3 (McKenzie-Johnson, 2004).

The composition of the landslide material has been determined by X-ray diffraction (XRD) and Scanning Electron Microscope (SEM) analyses (Bayer, 2006). Chrysotile asbestos fibers, derived from the serpentinite bedrock, comprise approximately 50% of the fine sediments being mobilized in the stream. Chrysotile from the landslide has been discovered in Sumas River deposits in Canada (Holmes et al., 2012). Other minor constituents from the serpentinite are chlorite, illite, and hydrotalcite. The matrix of fine sediments contains abundant gravel, cobble, and boulder sized serpentinite, conglomerate, and a variety of other rocks eroding out of the glacial till on the southern head scarp of the slide (Figure 4).

2.2 Human Health Concerns

2.2.1 Hazardous Material

Studies have determined that chrysotile asbestos concentrations exist at levels to be of concern (EPA, 2012). Longtime local residents, however, have expressed their concerns about this determination, claiming that there is no health concern (Melious, 2012). Meanwhile, there is contradicting research about the toxicity of chrysotile. Toxicological studies published in the Critical Reviews in Toxicology report that chrysotile fibers are rapidly attacked and broken down by cells, called macrophages, produced by the human body when foreign substances are introduced and therefore pose a low hazard (Bernstein et al., 2013). In contrast, the first toxicity studies involving rats comparing chrysotile from Swift Creek and Eldorado Hills, Colorado to the highly toxic Libby Amphibole from the Libby Mine, Montana was published in 2012 (Cyphert et al., 2012). This study showed evidence that the Swift Creek material was similar in toxicity to Libby Amphibole in rats, which was not the case for Eldorado Hills.

The risk to human health posed by the deposition of the asbestos material near human developments was evaluated using two different methods: one by the Washington State DOH and the other by the EPA. The DOH utilized historic records of cancer incidences for both mesothelioma, a cancer associated only with asbestos exposure, and for lung and bronchial cancers that can be caused by other influences and not solely by asbestos exposure. The occurrence of mesothelioma in the immediate Swift Creek area has been less than for occurrences in Whatcom County as a whole and in Washington State as a whole; this finding was also true for lung and bronchial cancer. The DOH, however, does not rule

out the possibility of chance and human error in this assessment because of the statistically small number of cases in the evaluation (DOH, 2010). They do not indicate that the presence of the chrysotile asbestos fibers elevate the occurrence of cancer.

The EPA took a field-based assessment and has shown that the asbestos fibers in the dredged landslide deposits could pose health risks to those who live, work, and play on or near the material. This was determined through activity-based sampling where a variety of activities that are typically performed in the area that would release particles into the air where they can be inhaled. In some cases, activities performed consistently over a lifetime increased cancer risks by at least 1 in 10,000, which is a regulatory threshold for the EPA. Some of the more intense and confined activities actually increased the cancer risk by 1 in 1,000 (EPA, 2006 & 2011).

In addition to airborne asbestos increasing the risk for cancer there are also health hazards stemming from the material deposited in streams. Heavy metals are released when aquatic organisms and acidic conditions break down asbestos fibers (Holmes et al., 2012); as a result the stream carries high levels of nickel, chromium, cobalt, manganese and magnesium. When released, these metals are transported into the Sumas River or work their way into municipal water supplies and into the food supply of humans, livestock and wildlife (EPA, 2006 & 2011, DOH 2010). Although a contaminant issue, the reduction of metals from the asbestos by means of aquatic organisms and acid treatment has been shown to soften and smooth the surfaces of particles, thus reducing their impact on human health.

2.2.2 Flooding

Another problem associated with the SCL is damage caused by floodwaters that deliver hazardous asbestos and heavy metals to down-stream floodplains (SCSMAP, 2012). Flooding redistributes potentially hazardous material to populated areas. Rapid aggradation of the streambed can promote flooding of Swift Creek. The large unvegetated surface of the landslide toe contributes to the flashy discharge and rapid swelling of the stream. The suspended material flocculates easily, increasing deposition and causing rapid aggradation of the streambed (Bayer and Linneman, 2010). This process along with high erosion rates from the toe and downstream South Fork reaches causes sediment build up in culverts, beneath bridges, and the low gradient reaches reducing stream conveyance.

Significant engineering challenges arise if channel avulsion and new channel formation occurs. If the stream abandons the historical channel it would likely disrupt long established boundaries, regulations, and natural resources such as fisheries and dedicated recreation areas. Floodwater flowing through agricultural fields into residential areas and nearby watersheds can deliver harmful wastes and chemical products where their presence is unwanted. Asbestos fibers can become suspended in air once dry and clean up or normal activities resume (EPA 2011).

These hazards generate management issues that are themselves problematic because of the constant effort required to mitigate flooding by sediment removal. Sufficient amounts of sediment can be removed from the stream channels to prevent flooding but it comes at the high cost requiring safe removal practices, storage space and the ultimate disposal of what is considered hazardous waste. A history of Swift Creek events and major mitigation efforts are found in Table 2.

2.3 Regulations and Responsibilities

There are several governing bodies within the regulatory framework at the federal, state and county level that all have an obligation to protect the health and welfare of the citizens and environment within the boundaries of the Swift Creek watershed and the downstream areas that are also impacted. A detailed explanation of the applicable regulations and policies at each level exists in the Whatcom County SCSMAP and is summarized in Table 3. Appropriate economically sustainable, long-term solutions must be utilized to reduce damage to property and resources. Research has been an important part of gaining understanding of the watershed processes and the full potential of health hazards.

2.3.1 Mitigation plans

Active and passive management strategies have been and are under development in order to fulfill the objective of managing sediment, flooding and human health (SCSMAP, 2012). Active approaches take into consideration the management zones that have been identified during previous research and include actions that are appropriate for each zone. Passive approaches have a broad application stemming from planning and managing the watershed as a whole.

Active management approaches have been primarily focused on the lower reaches of the watershed from the Canyon Reach down to the Oat Coles Reach and beyond (Figure 2). These involve construction projects such as bank armoring, in-stream traps and basins, channel maintenance and infrastructure repair. Actions involving the Upper Watershed include landslide related activity such as surface drainage and efforts to stabilize the landslide toe.

Passive management approaches involve long-term planning, monitoring and information dissemination. Some of the prevalent strategies listed in the SCSMAP are flood management planning and hazard identification, acquisition of key floodplain property, direct monitoring of landslide activity, sediment release and storage, effects of sediment deposition on the creek channel, flood and contamination education, and emergency response plans.

2.4 Stream Monitoring

The United States Geological Survey (USGS) monitored the sediment transport of Swift Creek with a gauging campaign on Sumas River, beginning in 2010 through September, 2013 (Magirl et al., 2011). Three gauging stations have been established along the Sumas River proximal to the Swift Creek-Sumas River Confluence at Massey Road near Nooksack, South Pass Road at Nooksack and near the town of Sumas, WA (Figure 1). Monitoring details, preliminary status reports, and data can be viewed online (http://wa.water.usgs.gov/projects/sumas/). By gauging the Sumas River before and after the confluence, the inputs of sediment from Swift Creek can be determined. The steady flow of the Sumas River is favorable for collecting discharge and turbidity data. One of the limiting factors to determining accurate sediment yield estimates is the upper limit of the turbidity sensor: the landslide has produced much higher turbidity levels than can be recorded by the sensor deployed for this research at 1600 Formazin Nephalometric Units (FNU), and higher than what was deployed by PSE at 3000 FNU. The USGS has also responded to this by deploying two sensors: a low level 3000 FNU sensor and a high level 10,000 FNU sensor to capture the peaks.

There are many other units to describe turbidity that characterize the detector geometry and light source of the sensor (USGS, 2013). Another turbidity unit that is commonly used in this type of research is the Nephalometric Turbidity Unit (NTU). Sensors that would be specified as FNU and NTU both have the same detector geometry with respect to the incident beam. The difference is that FNU sensors employ a light source in the 780-900 nm range, whereas NTU sensors employ a light source in the 400-680 nm range.

In addition to turbidity sensors, the USGS used some of the same types of equipment used in my research such as the ISCO water sampler and Forest Technology Systems DTS-12 turbidity sensors. At South Pass Road the station is equipped with an Analite 180 turbidity sensor that has a maximum turbidity limit of 30,000 FNU, twice the level of the DTS-12. This station also has an Argonaut SW shallow water flow sensor to monitor continuous water velocity for discharge measurements.

The USGS monitoring of Swift Creek along the Sumas River contributes to the Whatcom County SCSMAP by providing reliable and long-term data and professional analysis. The conditions of the Sumas River are more stable than Swift Creek and promote better turbidity data and a consistent cross section for discharge calculations. These data, along with meteorological data, are specifically useful in determining the effects of storms and the patterns of sediment release from the landslide toe and lower reaches of the creek. The physical water samples are analyzed for asbestos, heavy metals and sediment concentration. The Sumas River flows northward into Canada and therefore provides a larger context for the impacts of Swift Creek sediments and heavy metals on other communities, resources and ecosystems.

The PSE study was commissioned by Whatcom County to collect baseline sediment yield data at a location near a proposed site for sediment basins. The ultimate goal was to determine, if possible, the length of time the proposed sediment basins would take to fill. Studies such as the USGS and PSE studies are part of the passive strategy that governs the enactment of active management so that responsible and effective decisions are made.

The PSE project was conducted between November 2011 and April 2012 and used equipment and methods similar to what I used in that turbidity and discharge measurements were collected along with physical samples in order to determine a sediment yield. In the PSE study a flume was constructed to maintain a survey datum for discharge calculations. The stream gauging station was positioned about 1 km upstream of my stream-gauge site at the Goodwin Road Bridge (Figure 1). The creek at this point has a steeper gradient and is therefore more energetic and turbulent which caused problems during data collection.

2.4.1 Turbidity Threshold Sampling Background

Turbidity Threshold Sampling (TTS) methods were mainly developed by the Pacific Southwest Research Station of the United States Forest Service to produce reliable and accurate sediment yield estimates (Lewis and Eads, 2008). The TTS method employs a turbidity sensor, a water sampling pump to collect discrete water samples to analyze for suspended sediment concentration to relate to turbidity. The benefit of these methods to researchers is that continuous monitoring of turbidity captures the sudden and short-lived sediment pulses that would be missed with periodic monitoring. Turbidity sensors continually measure the scattering of light in water and can be used as a proxy for sediment concentration because light scatters more in water with higher sediment loads than water that is clear, the light scattering is directly proportional to the amount of suspended material

in the water. Turbidity has inherent challenges because the proportionality can change with sediment concentration, sediment size and water chemistry, which can all change during a monitoring period.

The turbidity sensor is interfaced with a water pump that will draw a physical water sample when triggered by a program in the turbidity sensor data logger during changing turbidity levels. The levels at which the pump is activated are known as thresholds. The researcher can set turbidity thresholds that maximize sampling during turbidity fluctuations and minimize sampling during stable turbidity levels. The thresholds take some time and expertise to appropriately designate; otherwise too many or too few samples will be taken. Once thresholds are set up and appear to be appropriate, the collection can be left to itself with periodic collection and maintenance.

To add interpretability to the turbidity data, researchers also collect discharge and meteorological data such as precipitation and temperature. Turbidity data by themselves can be difficult to interpret and these extra data are insightful for determining whether spikes in turbidity data are erroneous or are reacting to unexpected conditions. It is common practice to remove turbidity spikes that are not caused by suspended solids (Lewis and Eads 2008, Manka 2005, Meadows 2009). This allows researchers to examine how suspended sediment load is affected by changes in discharge and the relative timing and magnitude of sediment flux to storm related discharge.

2.6 Modeling Background

2.6.1 DHSVM Background

I used the DHSVM to model discharge for the Swift Creek in order to produce reliable, continuous hydrographs in my analyses and sediment yield estimates. The

DHSVM is a complex hydrologic numerical model designed to investigate hydrology, soil, and vegetation dynamics. It was originally developed by researchers at the University of Washington and the Pacific Northwest National Lab for hydrologic studies of forested mountainous watersheds (Wigmosta et al., 1994). The model calculates the energy and mass balance for each grid cell based on the physical relationships between the water in the soil, vegetation, and atmosphere (Figure 5). Gridded GIS data allow the model to accurately represent the inherent spatial heterogeneities that define the natural characteristics of a mountainous watershed. Meteorological inputs are distributed spatially at the DEM resolution and physical relationships are used to simulate evapotranspiration, snow accumulation and melt, infiltration, subsurface flow, runoff, and stream-flow processes.

Land-cover is divided into a two story canopy, the overstory and understory, and the soil. Correspondingly, there is a two-layer rooting zone reflecting rooting depths of the over story and understory. Movement of all precipitation through fall, snowmelt, and stem flow that infiltrates into the soil is based on Darcy's law (Wigmosta et al., 1994). The dominant vegetation type is used to estimate leaf area index, which directly affects evapotranspiration (ET). ET is estimated using the Penman-Montieth method. If infiltration exceeds ET and subsurface flow, the model predicts saturated overland flow directly feeding the stream channel. Essentially, water can leave a grid cell via direct evaporation, transpiration from vegetation, saturated subsurface flow, and saturated overland flow. The amount of mass exchanged between cells is calculated simultaneously for each cell. The effects of landcover changes can be explored by comparing changes in ET compared to changes in discharge (Vanshaar and Lettenmaier, 2001).

3.0 RESEARCH OBJECTIVES

The primary goal of my research was to correlate turbidity to total suspended solids being derived from the toe of the Swift Creek Landslide and to estimate the sediment yield during the monitoring period. This is important because the magnitude and variability of sediment flux has an impact on management plans. I designed and mobilized a stream gauging system from which to implement the Turbidity Threshold System (TTS) to collect turbidity data and physical samples to analyze for total suspended solids (TSS). I measured stream discharge from which to calibrate the hydrologic model and to calculate the sediment yield with. I used the calibrated hydrologic model to produce a continuous discharge from meteorological data using DHSVM.

A secondary goal was to compare methods of data analysis for estimating sediment yield from sediment concentration and discharge data. The PSE study was performed in a similar fashion to mine yet had significantly different results; I therefore used the data I collected and data from PSE in order to compare sediment yield estimates and to investigate differences in analysis procedures and the effect on the sediment yield estimate outcome.

4.0 METHODS

Correlating turbidity to total suspended solids and to streamflow is important in environmental monitoring, particularly when the sediment is damaging to public health and utilities. Methods consist of field data collection, lab analysis and computer modeling. Specifically, I collected in situ streamflow, turbidity and meteorological data. Furthermore, I collected physical stream samples to be analyzed for the concentration of suspended solids. I used a total of 15 discharge measurements and 30 water samples in my analysis. For the computer modeling element I used the DHSVM streamflow model for discharge and Excel reconstructions for TSS based on the physical data. This section discusses these methods in detail with a brief explanation of the methods used by PSE. The two studies used similar methods with a few key differences.

4.1 Stream Monitoring / Data Collection

Stream discharge, turbidity and sediment concentration analysis from physical water samples were key variables for my project. I collected data from Nov 14, 2008 to March 31, 2009 (4.5 months). For discharge I collected stream profile measurements and water velocity data during each site visit that conditions allowed. For turbidity and water samples, I designed and installed a system patterned after the United States Forest Service Pacific Southwest Research Station (Lewis and Eads, 2008) from the Goodwin Road Bridge (Figure 6). Three components were included as part of this station: a bridge-mounted submersed turbidity sensor, a physical water-sampling unit and a stilling well. The turbidity sensor and water uptake hose were suspended from the bridge on a hinging arm that allows destructive debris to pass underneath. The engineered system was intended to record river stage and turbidity continuously while taking discrete water samples at targeted changing turbidity

levels; this methodology is known as Turbidity Threshold Sampling (TTS). Turbidity was collected continuously but the water samples were collected periodically by the pump and by hand during site visits.

The physical water samples are analyzed in a lab for suspended sediment concentration (SSC) or total suspended solids (TSS). TSS was considered a close approximation for SSC in this basin to maintain consistency with the PSE study. The difference between TSS and SSC is the presence of organic particles along with sediment. The TSS record is correlated with the turbidity record to obtain a turbidity sediment rating curve from which to derive a continuous suspended sediment record.

4.1.1 Gauging Station Location and Equipment

My gauging station was located about 2 km downstream of the confluence between the north and south fork of Swift Creek (Figure 1) on the Goodwin Road Bridge, which marks the end of the Goodwin Reach (Figure 3). The flow is less turbulent at this location than further upstream as the creek progresses onto more level parts of the alluvial fan with a 1% gradient. The lower topographic relief of the fan results in a lower energy regime that deposits finer sediments: mainly sand, silt, and flocculated landslide material. However, the creek is at times energetic enough to transport coarse gravel and cobbles due to its flashy nature. A potential gauging site about 1 km upstream on GWL's log bridge was considered but was not used primarily because the higher gradient and the presence of boulders. The Goodwin Road Bridge site has less turbulent flow, smaller debris, easier accessibility, a solid mounting platform, and a secure location to mount a stilling well on the engineered banks supporting the bridge.

The TTS instrumentation was mounted following the methods of Lewis and Eads (2008) and guidelines from Forest Technology Systems (FTS), the turbidity sensor manufacturer, Appendix A. The turbidity sensor and water pump tubing were suspended into the water by a pole hanging vertically from a boom that extends 2 m horizontally from the bridge (Figure 6). This assembly was designed to allow the sensor to hinge in the direction of water flow, alleviating pressure from changing water velocities and allowing objects to safely pass underneath.

Instruments at my station included an ISCO 3700 water-sampling pump to collect 24, 500 ml raw water samples. Turbidity was recorded by a DTS-12 SDI Turbidity sensor and logged with an FTS HDL1 data logger. The FTS HDL1 sensor triggered the ISCO 3700 when the sensor detects rapid and sustained changes in turbidity. The ISCO 3700 and FTS data logger were contained in a weatherproof housing attached to the side of the bridge along with a 12 volt battery for power (Figure 7).

I made point discharge measurements following the USGS mid-section method using discrete stream velocity data collected with a Marsh McBirney Flo-Mate velocity probe (Rantz, 1982; Young 1950). The use of the mid-section method requires water velocity measurements at a constant interval across the channel with an accurate cross section. In order to accurately replicate the cross section at each field visit, I fixed a section of rebar into the north and south banks from which to suspend a metric measuring tape to guide the measurement interval. I recorded water depth and velocity every 30 cm. In the mid-section method, the cross section is divided into rectangular subsections that are centered on each measurement interval. The velocity measurement is the mean velocity of the subsection and

the water depth is the mean depth of the subsection. The discharge is calculated for each subsection and the sum of all the subsections is the total discharge of the stream.

4.2 DHSVM

The DHSVM is used by a wide body of researchers to model basin hydrology. Meteorological and geospatial data that characterize the soils, vegetation, and terrain are inputs in the model and are used to produce a simulated streamflow that represents observed streamflow. This requires altering parameters that affect the timing and delivery of water to the stream. The parameters with the largest effects on calibration are lateral hydraulic conductivity of the soil, soil thickness and precipitation lapse rate (Wigmosta et al., 1994).

I used ArcGIS 9.3 to develop the spatial data required to model the extents and physical characteristics of the watershed. Geospatial inputs include a digital elevation model (DEM), soil type, soil thickness, landcover, and a stream network. Meteorological data from a fixed station are spatially distributed in DHSVM at the scale of the DEM and adjusted for orographic and adiabatic processes. The spatial data are accessed online from government agencies such as the USGS, USDA, and NOAA. Step by step instructions to set up the streamflow model are provided in Appendix C.

4.2.1 DHSVM Streamflow Set Up

Digital Elevation Model (DEM)

The DEM is the foundation for the model, and all other inputs are based on the resolution of the DEM. I used the DEM to create aspect and slope grids in order to derive streamflow paths and to define the watershed boundaries. Topography is an important variable in receiving solar radiation and precipitation. The model uses the DEM in

conjunction with user defined temperature and precipitation lapse rates to calculate the increased precipitation rates at higher elevations due to adiabatic processes.

The DHSVM is commonly run with 30 m or larger pixel size. I used a USGS 10 m DEM because of the smaller size of the basin and size of the landslide within. A 2 m LiDAR data set was also available for this area but I chose to use a 10 m resolution to decrease computing time. Future studies may benefit from using the LiDAR data, however, because it can characterize the land surface better than DEMs.

Streamflow

The principal process of streams is to drain water from the basin and DHSVM uses stream flow measurements as the foundation basis for calibration. An Arc-Macro-language (AML) script provided by researchers from the University of Washington creates a stream network for the basin using the DEM. The GIS calculates flow direction of surface water based on the DEM to establish the stream channels. The streams are represented as segments, each with specific channel width and depth (Wigmosta et al., 1994).

Soil Thickness

The soil thickness is important to the basin's capacity to store water. The same AML that created the streamflow model also creates a soil thickness grid. This script uses a regression technique to estimate minimum and maximum soil depths based on slope and flow accumulation (Chennault, 2004). Soil thickness determined by the AML is difficult to verify and the predicted thickness of the landslide does not represent the actual thickness of the landslide. Matching the predicted thickness to the actual thickness is not critical to the streamflow calibration results in the end because soil thickness is adjusted during calibration to create streamflow results that best reflect measured data.

Soil Type

The hydraulic properties of soil influence the infiltration and movement of water through the soil. I used soil type data from the STATSGO (2001) database compiled by the U.S. Department of Agriculture. The soils in the Swift Creek basin are primarily a silt loam with varying concentrations of gravel, from very gravelly to no gravel. The landslide material is unique and is not included in the STATSGO data, so I developed a new soil type with the hydrologic and mechanical properties of clay to represent the landslide materials. The material was previously described as smectite clay due to the particle sizes (McKenzie-Johnson, 2004).

Vegetation

Vegetation types vary in their influence on basin hydrology due to their capacity to remove water from the soil through transpiration, precipitation interception, leaf drip, stem flow and evaporation (Keim and Skaugset, 2003). I used spatial vegetation data from the NOAA 2001 land-cover database to create a vegetation map of the Swift Creek basin. I adapted the vegetation data to reflect the unvegetated toe of the landslide.

Logging is and will continue to be an active process in the basin, but I did not examine the influence of logging in my study. Decreased evapotranspiration from deforestation can cause an increase in soil saturation, often causing slope instability and increased erosion from overland flow (Vanshaar et al. 2002). The landslide area was once dense old growth coniferous forest mostly of Douglas fir. Remnants of this forest still exist in pockets in the center of the landslide where the surface has remained undisrupted by landslide motion.

Meteorological Data

The meteorological (MET) data required as input include precipitation, temperature, wind speed, humidity, and short and long wave solar radiation. I used MET data from the Lawrence Station, commissioned in 2008 and maintained by Washington State University (Figure 1). It is located near the Swift Creek basin and provides longer term data with established quality control procedures before becoming publically available online. The only input missing from this station is longwave radiation, which was calculated using empirical and physical equations.

4.3 Model Calibration and Validation

Having valid streamflow predictions from the DHSVM was essential to my study. Computer models require calibration and validation using trusted multi-season data to verify the model variables that will produce correct results from year to year. I adjusted the DHSVM streamflow by modifying critical hydrologic parameters such as precipitation lapse rate, soil thickness, soil type, and lateral hydraulic conductivity until the simulated discharge closely approximated the measured discharge. Because I only had 17 discrete discharge measurements spanning four months at my Goodwin Road Bridge site, I was limited to a qualitative comparison of the predicted streamflow to the measured streamflow (Figure 8).

To improve confidence in my model I created another DHSVM streamflow output from the pixel that represented the position of the PSE stream gauge (Figure 1) to compare to the PSE calculated discharge (Figure 9). The DHSVM underpredicted the PSE discharge data with the settings that I used in my initial setup. I improved the fit to the PSE data by slightly increasing the precipitation lapse rate, leaving all the other variables unchanged.

With the modeled output using the refined settings, I performed a Nash-Sutcliffe quantification to determine the closeness of the model to the PSE data. The Nash-Sutcliffe efficiency and coefficient of determination numerically estimate how well the predicted data matches the observed data. The efficiency (E) ranges from $-\infty$ to 1 and the coefficient of determination (r^2) values range from 0 to 1; the closer the values are to one, the better the model fit. The method works for continuous data sets like the PSE discharge data but not using point measurements (Krause et al., 2005). Using the changes previously mentioned the model achieved an E of 0.817 and r^2 of 0.816. This was possible for the PSE discharge because their data were continuous in time whereas my data were only point measurements. I continued using the new settings in the DHSVM because they achieved the closest fit to both data sets.

4.4 Data Analysis

4.4.1 TSS Lab Analysis

I analyzed physical water samples for TSS at the Western Washington University Institute for Watershed Studies, a state certified water quality lab. The samples were collected by the ISCO 3700 and by hand at each visit. The TSS was measured by drawing an aliquot of known volume from the sample after adequate mixing. The landslide material flocculates and settles quickly, necessitating rapid sampling. I submersed a pipette to the center of the bottle during agitation so that a well-mixed sample could be drawn immediately. The aliquot was filtered, dried, and weighed. Each crucible was weighed three times before and after the addition of sediment. The average of the three dry weights of the clean filter was subtracted from the average of the three dry weights after filtration; the difference was divided by the volume of the aliquot to determine the concentration of

solids. The measured weights of each crucible were within 1 mg of each other. To verify the process, one water bottle would be sampled twice for TSS calculations. The repeated measurements were always within 3% of each other. I produced two relationships with the TSS data by pairing them with turbidity and discharge with the same time stamp. I used these relationships to form two continuous time series of TSS from which to derive sediment yield (Lewis, 2002).

4.4.2 Analyzing Turbidity Data Quality

Turbidity data were collected to serve as a proxy for TSS and generate a continuous sediment concentration time series. In order to create a time series, the turbidity data need to be examined for quality and erroneous data removed (Figures 10-13). Outside influences on the turbidity sensor, such as turbulence, debris, sunlight, and sensor position/orientation, affect the turbidity record. For this reason it is common practice to edit turbidity by either adjusting existing spikes to realistic levels or removing spikes that were not caused by sediment concentration. It is important, however, to exercise caution in order to avoid erroneously adjusting real data spikes.

The cause of individual turbidity spikes is not always obvious, so I established turbidity spike acceptance criteria based on the typical patterns of turbidity data, the relation to supporting data and knowledge of typical pitfalls associated with turbidity sensors in the field. The easiest way to verify a turbidity spike is with the presence of precipitation and coinciding changes in discharge, although this does not guarantee that the recorded turbidity levels represented what actually occurred. When reviewing turbidity data, the foremost consideration is the conformance of turbidity data to the typical pattern as explained in the following Turbidity Analysis Sequence and Criteria section.

My data contained turbidity spikes that were unexplainable by precipitation yet followed the typical turbidity pattern. I considered these spikes as possible random mass wasting events from the landslide toe and stream banks. Turbidity spikes from these sources appeared relatively small, sharp and narrow in the data, with typical peaks of around 200 FNU and lasting less than two hours. Another possible reason for no-precipitation spikes is that the sensor may have recorded errant data due to various types of fouling. The main types of fouling I experienced at Swift Creek were bubble fouling, surface interference, icing and sedimentation (or burial).

Turbidity Analysis Sequence and Criteria

I used the following steps when reviewing turbidity data to help ascertain whether peaks were real or due to fouling. Establishing these steps improved consistency throughout the analysis.

Step 1: Make separate plots of turbidity with discharge, precipitation and temperature.
Step 2: Identify known data segments in which the turbidity sensor was not working properly (dead battery, buried, or frozen sensor, etc.).
Step 3: Check each turbidity peak or connected sets of peaks for conformance to turbidigraph shape using the following criteria (Lewis and Eades, 2008).

- General criteria - Rapid rise, exponential decay.
- Precipitation related criteria – rise begins with precipitation, peaks prior to corresponding hydrograph, declines more steeply than hydrograph, response to multiple precipitation spikes during a storm.

Step 4: If a turbidity peak cannot be explained by precipitation or other corresponding data consider random mass wasting.

- Mass Wasting criteria – same general criteria but typically found during the discharge recession and sometimes after a freeze and thaw.

Step 5: If a turbidity peak is not explained by criteria in Step 4 or 5, consider known turbidity sensor pitfalls. The main pitfalls that were exhibited at my gauging station were bubble fouling, surface interference, icing and burial.

Characteristics of Observed Fouling

There are several ways in which the instrument may be fouled, causing the data to become suspect (Lewis & Eads, 2008). I list the types of fouling that were dominant in my data collection along with explanations of their type characteristics.

Bubble Fouling – During increasing streamflow and high water, excessive turbulence from the sensor housing and streambed cause bubbles that reflect light in much the same way as sediment. The effect of bubble fouling is typically high frequency, low amplitude noise.

Surface interference – There were instances that the sensor was too close to the surface when the streambed height and streamflow created a water height that was at the same level as the hanging sensor but not necessarily causing excessive bubbles as explained previously, but related. These conditions can increase the recorded turbidity values more than the sediment concentration and introduce erratic changes in turbidity. During these conditions, bubbles also occur from the sensor housing that cause bubble noise in addition to elevated and noisy surface interference.

Icing – Freezing conditions occasionally caused ice to form on the sensor optics. Icing typically caused a sudden increase in turbidity with a unique exponential change before suddenly dropping to pre-icing conditions.

Burial – Changing streambed morphology on occasion caused the sensor to rest on or near the streambed. During these occasions the bed load results in a very noisy pattern.

4.4.3 TSS-Turbidity and TSS-Discharge Relationships

In order to create the desired continuous TSS data I developed equations to relate Turbidity-TSS (Equation1) and Discharge-TSS (Equation 2) by plotting measured TSS against the quality-checked turbidity and the DHSVM discharge in separate graphs (O'Connor et al., 2011, Lewis and Eads 1996, Manka 2005, Figures 14 and 15). In the turbidity relationship, the suspect turbidity data and the discrete TSS data that corresponded in time were not used. For instance, the turbidity sensor during January 1 - 14, 2009 was violently erratic during the high streamflow conditions, so these data and the TSS measurements from the same time period were not included in the regression. The regression equation was used afterward to estimate turbidity peaks within "No Data" gaps as with the December and January storms (Figure 11).

2008-09 Turbidity-TSS Relationship

Modeled TSS = 2.0225T + 15.381 (1)

$R^2 = 0.85$

TSS (mg/L)

T (FNU)

2008-09 Discharge-TSS Relationship

Modeled TSS = 90.893Q + 662.51 (2)

$R^2 = 0.88$

TSS (mg/L)

Q (cfs)

I produced two sets of hourly TSS data for comparison using the Turbidity-TSS and Discharge-TSS relationships. These modeled TSS data were used to calculate sediment yield. I compared the results from both the turbidity and discharge to verify the two methods, however, the TSS analysis and comparative study were carried out using the Discharge-TSS relationship.

4.4.4 Estimating Sediment Yield

The sediment yield is the sum of the sediment load over a period of time. I formatted the predicted TSS into hourly time-steps to match the DHSVM discharge time-step. For each time-step I multiplied my predicted TSS from the Discharge-TSS relationship mentioned in the previous section with modeled discharge from the DHSVM. The summation of the hourly sediment loads equates to the estimated yield following Equation 3 (Meadows 2009). Detailed instructions for producing yield estimates are found in Appendix B and the Excel spreadsheet with calculations is on the CD included with this thesis.

$$L = \sum_{i} \left(t \cdot q_i \cdot C_i \right) \quad (3)$$

L = Sediment Yield (mg, convert to kg by dividing by $1x10^6$ mg/kg)

t = Time-step (hrs)

q_i = Discharge of Swift Creek (L/hr)

C_i = Total Suspended Solids (mg/L)

4.5 Comparative Study

A significant part of this document is the comparison of my data, methods and analysis techniques to those of a similar study conducted on Swift Creek (PSE, 2012). Whatcom County Public Works hired PSE to monitor the stream for the winter season of WY 2012 in order to quantify the suspended sediment yield. To accomplish this they collected water level, turbidity and TSS data from Oct 12, 2011 to April 6, 2012 (5.75 months). Their data collection methods were similar to mine but had the distinct advantage that they recorded continuous streamflow data through the interval. Despite this, they also experienced difficulties recording accurate turbidity measurements. The investigation was in response to the SCSMAP – Phase 1 conceptual design of the proposed sediment basins. In addition to offering a second sediment yield data set, the PSE study also provided a crucial additional set of discharge data from which to qualitatively verify the DHSVM hydrologic model (PSE 2012).

4.5.1. PSE Gauging Station Location and Equipment

The PSE consultants constructed their monitoring station approximately 1 km upstream of the Goodwin Road Bridge, near the fan apex (Figures 1 and 2). The sensor suite utilized by PSE was an ultrasonic level sensor and a Hydrolab MS5 Multi-Parameter

Sonde with a Stevens DL3000 datalogger. The stream at this location has a steeper gradient, between 4-5%, and a rougher bed containing gravels, cobbles, and boulders than it does at the Goodwin Road Bridge where my gauge was located. They constructed a concrete flume in line with the existing gradient that was designed to pass bed load while helping to control water level measurements and provide a consistent stream cross section (Figure 16).

Accurate discharge measurements are important in stream studies. The PSE consultants used empirical Mannings Equations (Equation 2) to calculate discharge from water level measurements over the flume. An ultrasonic level sensor was mounted on a log suspended directly over the flume. The flume provided a constant vertical datum with a known separation between the sensor and the flume. The water depth is the difference between the distance to the water surface from the sensor and the height of the sensor above the flume. The water depth was used to determine the area of flow and the wetted perimeter of the stream bank as a function of depth. See PSE (2012) for a complete set of the equations.

$$Q(t) = \left(\frac{1.49}{n}\right) A(x) \left(\frac{A(x)}{P(x)}\right)^{2/3} S_0^{1/2} \quad (4)$$

Q(t) = Discharge of Swift Creek (cfs)

n = Manning's n value (0.011)

A(x) = Area Flow Cross Section (ft^2)

P(x) = Wetted Perimeter as a function of Depth (ft)

S_o = Longitudinal Slope of the Flume (0.03 ft/ft)

PSE collected turbidity data with the Hydrolab MS5 turbidity sensor that would measure up to 3,000 FNU, which is twice what the DTS-12 that I used could obtain. The high turbidity level of the hydrolab was the primary reason for its selection. The Hydrolab was mounted in a galvanized steel pipe casing within the low-flow notch in the center of the flume (PSE, 2012).

To obtain TSS data PSE hand collected water samples. They made efforts to collect samples during storm events whenever possible. No TTS methodology was used by PSE, which limited the number of TSS data points (PSE, 2012).

4.5.2. Processing and Analysis

The PSE gauging station was not set up to collect physical water samples to determine TSS. Their TSS data were derived from water samples that were collected solely by hand during field visits. Avocet Environmental Testing analyzed the water samples for TSS. The consultants collected 13 water samples but only six samples were used in the subsequent sediment yield estimate process, compared to the 30 samples used in my analysis.

The turbidity data that were used in the yield estimation were limited in quantity. When plotted with precipitation and discharge the consultants found that only the first two weeks of data were trustworthy. The unit had become clogged after the first large storm and was temporarily removed for servicing. The unit was calibrated and replaced multiple times during the remaining season, but the recorded data continued to behave erratically.

Because of the variability of quality of the different types of data, the evolution of PSE's sediment yield estimate followed a circuitous path. The consultants created Discharge-Turbidity and Turbidity-TSS relationships. The Discharge-Turbidity relationship

included only the first two weeks of turbidity and corresponding discharge data, which spans only part of the first major storm. They found the best correlation using a second order polynomial (Equation 5). They used this regression equation and their calculated discharge to create a full set of turbidity to span the sampling season. For the Turbidity-TSS relationship, the consultants paired only six TSS values with corresponding extrapolated turbidity data (Equation 6). The best fit for Turbidity-TSS was a linear regression, which they used to extrapolate continuous TSS for the entire sampling season.

PSE Discharge-Turbidity Relationship

Modeled Turbidity = $21.975Q^2+55.941Q$ (5)

$R^2 = 0.95$

Turbidity (FNU)

Q (cfs)

PSE Turbidity-TSS Relationship

Modeled TSS = 0.6937 T (6)

$R^2 = 0.43$

TSS (mg/L)

T (FNU)

The general steps that PSE used to calculate yield estimation were the same steps I used with my data following the summation found in Equation 3. The PSE consultants allowed me to examine their yield estimation spreadsheet to understand their methods. I

reformatted their data to hourly time-steps and applied their relationships to verify their results. I obtained the same sediment yield as in their report. A step-by-step outline of the process is found in Appendix B, and an Excel spreadsheet with calculations is on the CD included with this thesis.

4.6 Timing Characteristics

Timing characteristics of watershed responses are important in understanding basin hydrology. Reliable streamflow responses can be predicted in a basin based on the duration and intensity of rainfall. Turbidity is not directly tied to basin hydrology and does not react to precipitation in the same way that streamflow reacts to precipitation. Regardless, streamflow is often used to predict turbidity and precipitation could potentially be used as well. The timing of turbidity relative to hydrologic measurements could provide insight to sediment flux characteristic and give strength to yield estimates.

To validate the Discharge-TSS regression, I compared the timing of turbidity peaks to precipitation and discharge peaks to determine if there were reliably repeated patterns. To accomplish this, I delineated 16 storms in discharge and turbidity data from the USGS South Pass gauge on the Sumas River along with precipitation data from the Lawrence weather station (Figure 17). The South Pass gauge is located less than one km downstream of the Sumas-Swift Creek confluence and the Lawrence station is within five km of the gauge near the headwaters of the Sumas (Figure 1). I sampled the data from Apr 27, 2011 up to Apr 6, 2012 with a time gap between May 5 – Dec 26, 2011 due to summer time dry period and dredging operations in Swift Creek during the beginning of December. For several weeks prior to December 25th, there was a suppression of sediment entering the Sumas River from Swift Creek possibly due to dredging that was performed in Swift Creek during that time

(Pittman, personal communication, January 2013). December 25th was the earliest date that the turbidity data exhibited an expected reaction to changing discharge, as shown by Beckenhaled et al (2003) and Meadows (2009).

For the purpose of examining hydrograph timing, I used the 16 storms by their time of occurrence. The time of occurrence is the time at the end of effective water input minus the time at the beginning of effective input. The multi-peak hydrographs were split and considered separately. The first time-step of each storm was assigned a time of zero and each time-step thereafter increases by an increment of one hour. The response of turbidity and discharge often coincided in time but occasionally the turbidity responded first. In these cases, time zero for discharge was set to the same clock time of the turbidity first response even though the hydrograph had not reacted yet. The peak time for both turbidity and discharge was simply the time from time zero to the highest measured value. I plotted the peak discharge time against the peak turbidity time to assess the overall correlation (Figure 18, Table 4).

To compare the timing of precipitation and turbidity peaks, I did not need to delineate the storm period; however, I used the same time counting scheme with each time-step numbered sequentially to simplify the time comparison. In most cases I could easily determine which turbidity peak corresponded with a given precipitation peak and then determine the time lag. When the peaks were smaller and closer together, pairing precipitation and turbidity peaks increased in difficulty and probably introduced some subjectivity in the analysis. For each storm period I sampled as many of the peaks that could be paired. I plotted the peak precipitation time against the peak turbidity time to examine the correlation (Figure 19, Table 5). There were on occasion precipitation peaks

that did not elicit a response in turbidity so these precipitation peaks were not included. Likewise, there were several turbidity peaks that could not be attributed to precipitation so these peaks were not included.

I made an analysis of the magnitudes of the precipitation-turbidity pairs for the 2011-12 and 2012-13 seasons. I plotted the magnitude of turbidity against the magnitude of precipitation to see if a correlation existed that would allow precipitation to be used to predict the level of turbidity. Plotting all the pairs together did not produce any meaningful relationships so I divided the data up into two month durations to account for possible seasonal progression (Figures 20-22).

4.7 Modeled Fall-Winter Sediment Yield

Variability in weather patterns from year to year will influence the quantity and peak magnitudes of sediment eroding from the landslide. In order to examine variability in sediment yield based on weather patterns, I created several DHSVM hydrographs using my calibrated DHSVM streamflow model with Lawrence station MET data from Oct 1 to Mar 31 for the years 2009-2012. More seasons would have been included if the Lawrence station had been established earlier than 2008. I compared the cumulative seasonal discharge and the maximum discharge rates from these hydrographs. I applied my Discharge-TSS regression to each hydrograph to quantify estimated sediment yield for each season to examine the influence of cumulative seasonal discharge and maximum discharge rates on sediment yield.

5.0 RESULTS

The data from my 2008-09 study and PSE's 2011-12 study contain discrepancies and shortcomings that introduced significant errors to my comparative analysis. Among the most influential problems were limited streamflow data, equipment performance in rapidly changing streamflow, and different weather conditions. In spite of the weaknesses, both studies produced sufficient data that, when combined, produced noteworthy results. I utilized data from the USGS Sumas River, South Pass Road stream gauge to augment the objectives of my study to provide insight into the hydrology and sediment erosion processes of the basin.

5.1 Hydrologic Modeling Results

Creating a meaningful hydrologic model relies on valid, continuous, multi-season measured discharge. I made streamflow measurements and streambed profiles at nearly all my site visits, except when conditions were unsafe, and used these to produce a point discharge dataset for calibrating the DHSVM. On two occasions I made unscheduled trips in order to capture peak flows during storms.

The DHSVM discharge was thereby qualitatively calibrated using a limited point dataset (Figure 8). I was able to further refine the model using discharge from the 2011-12 PSE study, which used an engineered flume (Figure 9). I performed a Nash-Sutcliffe (1970) statistical analysis to quantify the fit between the DHSVM discharge and the PSE continuous discharge data as discussed in the methods. The efficiency ($E = 0.82$) and the coefficient of determination ($r^2 = 0.82$) values reflect a reasonable fit. The efficiency could have been higher, but there were two measured peaks that were significantly out of proportion to the low volume precipitation that occurred at those times. In the absence of

significant precipitation, the DHSVM did not simulate these peaks. By plotting the PSE discharge data with discharge data from the USGS South Pass Road gauge, I was able to verify the March peak and determine that the January peak was errant and likely caused by some malfunction of the flume/water level sensor.

5.2 Hydrology

As observed qualitatively over the years, seasonal precipitation in the Swift Creek basin has a large impact on the mobilization of sediment, and can be extremely variable. In this section I compare the precipitation and discharge of the major storms during my 2008-09 collection season and PSE's 2011-12 season to examine how differences in hydrology can impact sediment flux out of the basin. The precipitation results come from the Lawrence station precipitation data (Figure 23). My 2008-09 discharge results come from the DHSVM modeled discharge (refined using the 2011-2012 data). The 2011-12 discharge results come from the PSE calculated discharge (Figure 24).

5.2.1 2008-09 Precipitation and Discharge

My 2008-09 collection period at Goodwin Road bridge was from November 1, 2008 to March 31, 2009. During this time, the total discharge and precipitation was 4,500,000 m^3 and 40.31 cm, respectively. There were two major storms, each exhibiting a different discharge response to the relative amounts of precipitation, which in turn had an effect on sediment yield per storm. The first storm occurred in November, 2008 and the second occurring in January, 2009 (Table 6).

The storm beginning on November 1, 2008 was the smaller of two in terms of discharge even though it had the greatest precipitation. The hourly rainfall rate was 1.3 times that of the January storm and the total precipitation was 1.5 times greater. The peak

discharge, however, was only 64% of the January peak and the discharge volume that occurred was 94% of the volume occurring in January. The November storm yielded a 15% greater contribution to the total precipitation recorded during the sampling season, yet contributed 3% less to the total discharge recorded during the season (Table 6). This could be due to soil storage effects from being early in the rainy season. The January storm was also influenced by snow melt, which was an additional contribution to the discharge without precipitation. The November storm lasted 17 days while the January storm only lasted 6 days.

5.2.2 PSE 2011-12 Precipitation and Discharge

The PSE 2011-12 collection period was from October 12, 2011 to April 6, 2012. During this time, the total discharge and precipitation were 4,000,000 m^3 and 53 cm, respectively. There were three major storms recorded in the discharge data, however only two were verified to be real as previously mentioned in Section 5.1. The errant peak occurred in January 2012 and was the largest of the three in terms of apparent discharge. The first real storm of this season occurred in November, 2011 and the second real storm occurred in March 2012 (Table 6).

The storm beginning on November 22, 2011 was the smaller of two in terms of discharge even though it had the greater precipitation. The hourly rainfall rate was 3.8 times that of the March storm and the total precipitation was 2.3 times greater. The peak discharge, however, was only 82% of the March peak and the discharge volume that occurred was 91% of the volume occurring in March. The November storm contributed 6.5% more precipitation to the total precipitation recorded during the sampling season, yet contributed 1% less of the total discharge recorded during the season. As with my 2008-09

data, this could be interpreted as a soil storage effect due to being early in the rainy season. The November storm lasted 8 days while the March storm lasted only 3.

5.2.3 Cumulative Precipitation Comparison

I compared the cumulative precipitation between the two seasons to investigate differences in precipitation patterns and intensity (Figure 25). The plots for both seasons have similar average slopes for the duration of the season, the slope for 2008-09 is 0.36 and the slope for 2011-12 is 0.3. Each season has nearly identical average hourly rainfall for the duration of the gauging, 0.0121 cm in 2008-09 and 0.0124 cm in 2011-12 (Table 6). The cumulative plot for the 2011-12 season has a steady and consistent slope; however, the slope of my 2008-09 season is disrupted by large changes caused by the November, 2008 and January, 2009 storms.

5.3 Sediment Relationship with Discharge and Turbidity

I used two techniques for estimating sediment yield: one based on turbidity and a second based on discharge (Benkhaled and Remini, 2003; Chappell et al., 2004; Kunkle and Comer, 1971, Pfannkuche and Schmidt, 2003; Smith et al., 2003; Fenton 2006; Lewis and Eads, 2008). The sediment relationships with turbidity and discharge that are reported here were created for the entire sampling season. It is beneficial to create individual storm relationships to take into account seasonal changes that affect sediment erosion (Meadows, 2009); however, I did not have enough TSS samples per storm to create individual storm relationships. I used 30 water samples for TSS lab analysis. Of the 30 TSS samples, I paired 26 with turbidity for the Turbidity-TSS relationship. There were four TSS samples that were collected during times of poor turbidity data and could not be paired. The PSE

consultants created their sediment relationship in a different manner predicated on the quantity and quality of data they collected, as described in the methods section.

5.3.1 2008-09 Relationships

Turbidity-TSS Relationship

In general, my turbidity data were noisy and suffered from several types of fouling, yet there were significant periods of data that demonstrated that my sensor was working properly (Figure 26). My 2008-09 Turbidity-TSS relationship (Figure 14) was created from noisy turbidity. The turbidity contained anomalous rises in turbidity from January 15-24, 2009, and February 18-26, 2009 and were removed from analysis along with the noisy turbidity of the January storm (Figure 11). These removals along with other small adjustments account for 34.15 % of the raw turbidity data. The January 15-24th anomaly was likely caused by bubble fouling caused by high water turbulence (Figure 27). The February 18-26th anomaly could have been caused by bottom fouling and the progressive growth of the stream bank out and around the sensor (Figures 28 and 29).

Discharge-TSS Relationship

Sediment concentration does not directly follow discharge, but offers the most consistency and long-term projection potential. I created a Discharge-TSS relationship using TSS paired with the modeled DHSVM discharge. One shortfall of this relationship is a lack of TSS samples in the middle range of discharge data to use in the correlation (Figure 15). As such, the relationship is based on a cluster of points near the origin being forced into a linear form by a couple of high TSS, high discharge points.

5.3.2 2011-12 Relationship

The consultants from PSE employed a two-step process to relate discharge to TSS. First they related discharge and turbidity using a 2nd order polynomial. Although the correlation was good ($R^2 = 0.95$), they used only two weeks of data. Hence, when the polynomial is used to extrapolate into the full season, the model produces anomalously high turbidity values from discharge. Second, they developed a linear relationship between turbidity and only six TSS data points to get continuous TSS from the new turbidity dataset. Also, as previously discussed in section 4.5.2, the two weeks of data that they used in the model were collected from the rising limb of the hydrograph but the recession side of the hydrograph is equally important to fully assess the streamflow-sediment relationship. I believe these, collectively, are the likely sources of error for the anomalously high sediment magnitudes predicted in their study.

The first two weeks of turbidity data from the PSE 2011-12 study were considered to have the only valid Turbidity-TSS data pairs. I plotted these points along with my 2008-09 paired data for comparison (Figure 14). These PSE data fell within the scatter of my data, however, the slope of only the PSE Turbidity-TSS was less than half of slope for my 2008-09 data.

5.4 Sediment Yield Estimates

My sediment yield estimates were determined using the regression equations and procedures described in Section 4.4.3. In this section, I report total yield estimates in terms of mass in kg and sediment concentration in mg/L. I calculated two yield estimates: one using a turbidity based method, and a second using a discharge based method. My 2008-09 Turbidity-TSS model yielded 12,744,427 kg of sediment over the season, whereas my 2008-

09 Discharge-TSS model yielded 23,287,097 kg, almost double the results from the turbidity method.

An interesting observation on the timing of sediment flux during my 2008-09 season was that most of the suspended sediment movement occurs during the large storms. During my sampling season, 89% of the estimated sediment yield was delivered during the 9 day January 2009 storm. Following the storm only 6% of the total estimated sediment yield was delivered while 28% of the rainfall occurred. The maximum TSS value that I observed in my study was 20,686 mg/L, which occurred during the season's maximum discharge event beginning on Jan 6, 2009 (Table 7). My 2008-09 Discharge-TSS model predicted a TSS maximum of 22,065 mg/L, a 6.6% increase from the measured TTS. The maximum predicted hourly sediment load was 524,694 kg.

The PSE sediment yield estimates were determined using the regression equations and procedures described in Section 4.5.2. The 2011-12 sampling season yield reported by PSE was 111,527,000 kg, more than four times my discharge derived estimate and almost nine times my turbidity derived estimate. I only use the discharge generated estimate to compare to the yield estimate from PSE because of the ability to create streamflow data for other years using the DHSVM and archived precipitation data. This allowed me to make more direct comparisons and analyses between the estimate yields of two studies. The maximum TSS value that PSE observed was 13,500 mg/L, which occurred during the season's storm with the highest precipitation yet only the second largest verified discharge beginning on Nov 23, 2011 (Table 7). The PSE 2011-12 model predicted a TSS maximum of 310,564 mg/L, 23 times greater than the corresponding measured TSS. The maximum

hourly sediment load predicted by PSE 2011-12 model was 4,481,476 kg, 8.5 times larger than what was predicted for my 2008-09 data.

5.5 Cross Application of the Estimate Methods

As a matter of comparison, I applied my discharge based model to the PSE discharge and similarly, I applied the PSE model to my data (Table 7). When the PSE data were processed using my methods the TSS was 14,183 mg/L, only 4% of what it was when originally processed by PSE and only 64% of the maximum modeled concentration when using my 2008-09 data. The total estimated yield was 14,584,907 kg, 13% of the yield determined by PSE (111,527,000 kg). I processed my data following the PSE methods and the maximum modeled TSS was 608,576 mg/L, 28 times the concentration calculated using my methods and 1.9 times the modeled concentration of the PSE data. The total estimated yield for PSE data with their model was 341,488,348 kg, 17 times the yield determined using my methods (23,287,097 kg). These results from cross applying the estimation methods indicate that total actual sediment yield was greater in 2008-09 than in 2011-12, as would be expected given the record storm of January 2009.

5.6 Timing Characteristics

5.6.1 Peak Discharge vs. Peak Turbidity Timing

I relied on my Discharge-TSS relationship for my sediment yield estimate so I compared the timing of peak discharge to peak sediment concentration. I used the USGS South Pass Road discharge and turbidity data, considering turbidity as a proxy for sediment concentration. It is common for turbidity to rise and fall quickly and peak early, relative to the associated hydrograph (Lewis and Eades, 2008). I plotted the timing of peak discharge

against the timing of peak turbidity for each storm and there appeared to be a relationship (Figure 18). The regression equation has an R^2 value of 0.8015. On average, discharge peaks lag behind turbidity by 11.9 hours but ranges from one hour to 37 hours (Table 4).

5.6.2 Peak Precipitation vs. Peak Turbidity Timing

To further characterize the reaction of sediment flux in response to a storm, I compared the timing of peak precipitation to peak turbidity. I used 3.5 times more data points in this correlation than in the discharge correlation because of the multiple precipitation and turbidity peaks during a storm, whereas the discharge tends to have only one peak per storm. I plotted the timing of each precipitation peak against the timing of each turbidity peak that could be paired and the correlation is unreasonably good, which is likely due to subjectivity in pairing the peaks (Figure 19). The regression equation has an R^2 value of 0.994. On average, turbidity peaks lag behind precipitation by 4.2 hours but ranges from zero hours to 10 hours (Table 5).

5.7 Precipitation Magnitude vs. Turbidity Magnitude

Given the apparently close correlation in the timing between precipitation and turbidity, I also tested for a correlation between the magnitudes. I created scatter plots for the 2011-12 and 2012-13 winter seasons to investigate the possibility that turbidity peak magnitudes could be predicted by precipitation peak magnitudes. I used the USGS Sumas turbidity data and the Lawrence station precipitation data. There was no correlation in magnitudes over the season as a whole so I divided the season into two month durations to examine seasonal effects. For the 2011-12 season, there were significant correlations between the magnitudes with R^2 from 0.6 to 0.7 with an average of 0.66 (Figure 20). This was promising so I evaluated the 2012-13 season in the same manner. These correlations,

however, were poor with R^2 from 0.2 up to 0.4 with an average of 0.38 (Figure 21). Shifting the time durations forward by two weeks for 2012-13 yielded improvement in the correlations ranging from 0.1 to 0.7 with an average of 0.49 (Figure 22). A consistent pattern in the correlations for both seasons was an increase in the R^2 value from the first bracket to the last bracket of the season.

5.8 Multi-Year Modeled Sediment Yield

In order to provide insight about the variability of sediment from yield year to year, I used the DHSVM and my Discharge-TSS relationship to model sediment yield from Oct 1 to Mar 31 for the years 2008 through 2012. Using the DHSVM allowed me to take advantage of existing precipitation data from previous years to model discharge for intervals having no measured discharge. This technique will also be useful using predicted future precipitation outputs from climate models. In this exercise, the seasonal sediment yield corresponds to higher maximum discharge rather than the total discharge. The highest seasonal sediment yield was in 2009 followed by 2011, 2010, and finally 2012 (Table 8). The maximum discharge from year to year follows the same order (Table 8).

6.0 PROBLEMS ENCOUNTERED

Multiple factors played a role in limiting my ability to produce an accurate estimate of sediment flux delivered by the landslide including a lack of historical streamflow data, rapidly changing streambed morphologies, snow and freezing conditions and equipment malfunctions. Notwithstanding, my research project provides insight about sediment flux from the landslide within the Swift Creek watershed and lays a foundation for future work using the TTS methodology. Additionally, these same problems caused uncertainty in the calibration and validation of the DHSVM streamflow model. The uncertainty of this model, however, was improved by the 2012 PSE study which produced a 5.5 month sampling season with continuous discharge measurements using an engineered flume.

6.1 Stream Morphology and Discharge Measurement Problems

Monitoring Swift Creek is difficult due to its flashy nature, e.g., instruments have been temporarily lost in previous attempts (Bayer, 2006). The turbidity sensor, water sampler, and stilling well were all disrupted by weather and streamflow dynamics. The aggradation of the stream-bed and rapid changes in streambed morphology created gaps and false data.

I attempted to record stage data by constructing a stilling well on the side of the river channel at Goodwin Road Bridge. I used a Stevens Water shaft encoder and data logger to measure stage. A float and counter weight looped around a pulley on the shaft encoder pulley reacts to rising and falling stage and causes the pulley to rotate; when calibrated correctly this rotation equates to a linear vertical distance. It became evident within a few field visits, however, that the site was not suitable for a stilling well due to the lack of a stable vertical datum. The stage data ended up being of no value for two main reasons:

deposition along the stream bank would often redirect the flow of water away from the well, and the turbulent conditions at peak flows would derail the cable from the pulley allowing it to spin freely and record an endless stage change. As a result, no rating curve was established. I did not mention attempting to measure water level in my methods section because it did not work. I mention it here to help describe the difficulties that were experienced.

The streambed morphology altered the routing of water past the sensors, this was particularly problematic to the stilling well as the water would no longer be in contact with the well structure or the well would become clogged with sediment so that changes in the water level would not transfer into the well. I repeatedly dug out the well and flushed the system clear of sediment. Occasionally, high water turbulence would cause the float cable to derail from the encoder shaft pulley which would continue to spin and record an ever increasing or decreasing stage.

As with all streams, high water levels can be dangerous. Twice in the season, during the highest flows, I made streamflow measurements from the bridge because of unsafe conditions. Floating and submerged objects were observed striking the sensor housing. Even at medium flows when it was safe to enter the stream to measure streamflow, I was forcibly struck on my feet and shins by large debris, presumably small cobble size rocks and waterlogged branches (Figure 30).

I placed the turbidity sensor in the best position on the bridge to keep it in the stream as much as possible. Generally, the turbidity sensor stayed in the water but not always in the thalweg as the streams edges could grow laterally more than a meter over the course of a week, this caused the water depths under the sensor to decrease (Figures 28 and 29). For

instance, during a site visit on January 13th, I noted the streambed level had aggraded 16 cm during the previous seven day storm. I visited again on January 15th and noted that the streambed had incised 11 cm.

Interestingly, the stream banks would episodically encroach and then erode away from the sensor; however, during one visit in February, I discovered that icy sediment had grown out around the sensor when it had been nearly a meter away at my previous visit (Figure 29). As a result, I dug the sensor housing out of the sediment and re-routed the water to maintain a flow past the sensor and discourage bank regrowth; thus keeping the sensor in the water. When the sensor housing containing the water sampling hose is close to, resting on or buried in sediment, the turbidity becomes erratic and the water pump fills the sample bottles with previously deposited particles. No attempt to analyze the particle size distribution was made so the influence of this was not determined but it was assumed to happen on Feb 17, 2009 when the sensor and tube were buried.

6.2 Seasonal Challenges

In addition to stream morphology challenges interrupting the flow of water, freezing conditions occurred several times, causing the stream to freeze over completely. At times the temperature would drop below freezing for extended periods of time and ice would grow around the sensor. In December 2008, the whole river was frozen over with multiple layers of ice totaling about 15cm thick (Figure 31). On another occasion after ice had developed around the sensor, the water level dropped and the ice caved in. When this happened, the support stays that are anchored to the bridge could not support the weight of the ice and one of the anchoring eyebolts was pulled apart. The assembly dropped into the bed and became

partially buried. When I arrived to collect data there was still a block of ice the size of a small boulder attached to the sensor housing.

Freezing temperatures caused occasional problems due to unsafe conditions on the stream and ice formation on the sensor. When ice was built up on the stream I did not make discharge measurements because it was unsafe or impossible to enter the stream. This lead to some time gaps in my point discharge data, limiting my ability to calibrate the DHSVM streamflow. Also, the water line to the pump would occasionally freeze but this probably was a minor problem because the turbidity values were typically minute during these times and samples wouldn't be needed.

6.3 System Shortfalls

I encountered restrictions of the turbidity sensors design and operability. By design, the DTS-12 has a turbidity maximum limit of 1592.8 FNU. As previously mentioned, the actual turbidity in the stream repeatedly exceeded this limit and the peak turbidity could not be determined in these cases. I had to withhold valuable TSS samples that were collected during these data gaps from my correlations because there were no corresponding turbidity values. This was detrimental to the overall confidence of the correlations.

I lost the several weeks of TTS sampling after the initial installation. The FTS data logger is controlled by a TTS sampling program that contains code for the user to specify turbidity thresholds that will trigger the water pump to take a sample during changing conditions. The default threshold values were in place at the time of installation caused the sampler to fill all 24 ISCO bottles within the first few hours after deployment. I adjusted the thresholds two more times with guidance from FTS engineers to find the appropriate values for this sensor at the Swift Creek.

6.4 Modeling Limitations

Modeling the discharge with the DHSVM and the sediment flux has the advantage of a continuous time series but is only useful when properly calibrated to measured data. The flashiness of the stream is one of the biggest obstacles for collecting discharge data. I typically collected streamflow data once per week except on a couple of occasions when I sampled more frequently in order to better catch storm events, or the occasions that dangerous conditions existed and no measurements were made. My data were augmented by the PSE dataset that were graciously provided so that I could better calibrate the DHSVM model.

I make the assumption that all the solids contributing to the turbidity at my stream gauge come from the landslide toe. This is a fairly reasonable assumption because streams that drain the forested parts of the basin produce less material as can clearly be seen visually, but the extent of their contribution is unknown (Figure 32). During the January 2009 storm, significant amounts of sediment came from other parts of the basin. The effects of this event were seen in washed out tributaries of Swift Creek such as the Great Western Creek (Figures 3 and 33). Cutting into the streambed with a shovel after the high water subsided revealed layers of coarser grained, rusty brown to tan material that were indicative of the conglomerate beds rather than the gray sediment from the toe. The data from this storm were not used when creating sediment relationships because of poor quality turbidity data, effectively removing the extra sediment from the analysis.

7.0 DISCUSSION

The primary goal of my research was to estimate suspended sediment yield derived from the toe of the Swift Creek Landslide during the monitoring period of Nov 15, 2008 to Mar 31, 2009. An additional goal was to compare the techniques I used with those used by consultants from PSE who estimated sediment yield from Swift Creek during the 2011-2012 winter season using similar instruments and methods. While examining these data during my comparisons, I found that there were some predictable timing correlations between turbidity with precipitation and discharge that may offer insight into mass wasting processes on the landslide and for future sampling and modeling efforts.

7.1 Hydrology

My 2008-09 and the PSE 2011-12 seasons had similar overall discharge volumes but precipitation patterns were significantly different. My 2008-09 season had two high-magnitude discharge events lasting more than a week (Figure 24). The PSE 2011-12 discharge data were characterized by smaller, more consistent precipitation and discharge events that lasted only several days. This is most obvious in the cumulative precipitation plots where my 2008-09 season has large, sudden accumulations that are absent from the PSE 2011-12 data (Figure 25). The first significant November storms of both seasons had higher precipitation but lower resulting discharge than the later storms, which I attribute to groundwater storage.

Unfortunately, the effect of these precipitation differences on sediment load cannot truly be determined because of the lack of sediment data, particularly in PSE's 2011-12 data. It appears that large, intense storms that occur after a period of dry or frozen conditions produce the most suspended load. The storm containing the maximum sediment load in

2011-12 cannot be determined because the turbidity sensor no longer functioned properly after the November 2011 storm. During my 2008-09 season, the January 2009 storm delivered the largest amount of suspended load of the season, as indicated by both the turbidity and TSS data. The intensity and duration of the rain event following a period of snow accumulation in the basin help account for the measured sediment load because the stream experienced exceptional swelling which added a significant amount of sediment through re-suspension of the streambed and bank erosion.

7.2 Sediment Relationships

7.2.1 Sediment Relationship with Turbidity and Discharge

I used turbidity and discharge as proxies for sediment concentration in spite of data collection difficulties. I created relationships for both, but it was difficult to assess the quality of one over the other. Neither relationship was very rigorous because of the lack of sufficient TSS samples. The Turbidity-TSS relationship was considered low confidence and was not used in my analysis because the TTS method was hindered by field conditions. My turbidity data were generally noisy and I removed 34% of them from my analysis, although, there were stretches of turbidity data that I assumed to be accurate when plotted with discharge and precipitation (Figure 26).

The quality of the Discharge-TSS relationship was also reduced by inadequate discharge data. The DHSVM that I relied on for discharge data was not properly calibrated nor validated. In spite of the low confidence, I used the discharge relationship throughout my other analyses because there were no other sources of discharge and precipitation data to create additional sediment yield estimates. Moreover, because of the rapidly evolving morphology of Swift Creek, it is likely that modeling will be necessary to predict flows in

the future. I was able to increase confidence in the DHSVM discharge output by validating it against the PSE measured discharge, which was considered high confidence data on account of the engineered flume and optic water level sensor used to estimate the discharge.

7.2.2 Seasonal vs. Individual Storm Relationships

Seasonal relationships between stream discharge and sediment load are not considered to be as accurate as individual storm relationships because basin evolution and source area can cause differences in the quantity and character of sediment yield from storm to storm (Manka 2005, Sun et al., 2001, Kunkle and Comer, 1971). Seasonal (or annual) relationships have been documented in previous studies and compared to individual storm based relationships (Fenton, 2006; Manka, 2005; Kunkle and Comer, 1971; Brasington and Richards, 2000; Lewis, 1996; Lewis and Eads, 2008; Meadows, 2009). During my sampling season I was not able to collect TSS samples to the extent necessary to analyze individual storms, so a whole season relationship was the best possible choice.

There can also be different relationships between discharge and sediment during the rising and falling limbs of a storm (Manka, 2005), which was observed during my study (Figures 17 and 26). Manka compared the slopes of rising limb regressions to the slope of falling limb regressions from three gauging station within a watershed and found no seasonal bias, station bias or consistent pattern between the slopes of the rising and falling limbs. In some cases, the slope of the rising limb was higher than the falling limb; in other cases, it was lower. He produced an annual relationship for the three stations and compared the annual yield estimate to the estimates produced from the individual storm relationships. The annual relationship predicted higher sediment yield at two of the three stations and

lower at the third. The over-predicted estimates were 1% and 16% over the individual storm based estimate, the under predicted station was 8% less (Manka 2005).

Manka's findings further support the unpredictable nature of sediment delivery, from site to site, storm to storm, and from year to year; however, the percent differences between the seasonal and storm based estimates are not completely unrelated. Even though estimate methods for an entire season may be able to generate reasonable seasonal estimates, they are not useful for predicting sediment flux from individual storms (Manka, 2005). Manka applied the annual regression to specific storms and found that it can result in as much as 74% difference than storm based regression. A possible reason for this is that annual regressions do not account for changes that influence sediment flux such as the size of individual storms, frequency of storms, seasonal progression or the possible shifts in data collection sensors.

Manka's findings were important to consider while analyzing my data because they show that an annual estimate can be useful, while showing the importance of developing relationships for narrower time frames within storms over multiple seasons. Therefore, several more years of rigorous data collection at Swift Creek should be undertaken to refine sediment estimation models.

7.3 Sediment Yield Estimates

I found large differences between my discharge and turbidity estimates and the PSE estimates. My turbidity based estimate was only half of my discharge based estimate. There are three possible contributing factors that could explain this difference. First, using a linear model to predict sediment yield from discharge is likely not appropriate because it cannot address the variability of sediment concentration. For instance, storms of equal size and

duration may not produce the same volume of sediment because of the influence of previous storms. This has an impact on sediment yield estimates, but is not predictable by a linear model. My Discharge-TSS relationship had a significant gap due to sporadic TSS samples and discharge measurements, especially with values in the mid ranges from 5,000 mg/L to 15,000 mg/L for TSS and 30 cfs to 180 cfs for discharge (Figure 15). The large January 2009 storm produced such high discharge levels that a linear regression with a good correlation is forced even though at low levels there is no linear pattern. Had the TTS method been able to perform in the conditions during the storm and more TSS samples collected, a more appropriate regression may have been revealed.

A second concern is that the linear discharge model predicts increasing sediment with increasing base flow level over the season. The linear model forces sediment concentration to reflect discharge, therefore, as the base flow increases from one storm to the next the sediment concentration also increases. In reality, the sediment concentration should drop to near zero after the storm sediment slug passes as the stream flow returns to base flow levels.

A third problem is that the linear discharge model cannot account for random mass wasting and sediment flux events not caused by precipitation. Random mass wasting events occasionally occur on the landslide toe, independent of precipitation. Moreover, not all sediment in the stream is mobilized by raindrop detachment and overland flow. Some sediment is mobilized as increasing discharge re-suspends channel sediment and erodes stream banks, which can also be independent of precipitation through snow melt. Increasing discharge during the rising limb brings a slug of suspended sediment downstream from in-channel stored sediment. Once the slug passes, there is a shift in the source of sediment

from the stream pockets to the un-vegetated toe. As the flow decreases, the flocculation and rapid deposition of suspended sediment takes place in eddies, backwaters, and other low velocity areas with some sediment ending up on the banks above low-flow conditions until the next high flow (Pittman 2013 personal communication, January 2013).

These same problems exist with the PSE relationships but were compounded by their inadequate sediment-yield relationships. First, they created a Discharge-Turbidity relationship using only two weeks of data fitted to a 2nd order polynomial. In doing so, they assumed that these two weeks of data were representative of the entire season. They created a complete turbidity data set from this regression, which yielded some excessively high turbidity peaks. To complete the sediment calculations, they created a linear Turbidity-TSS relationship data set based on only six Turbidity-TSS pairs that were spaced throughout the season. In essence, they used less than 10% of their measured data. As a result, the relationships they used greatly over predicted the sediment yield for their season. A contributing factor could also be the inclusion of what appears to be an erroneous discharge peak on January 21st, 2012 as discussed in section 5.2.2.

The disparity in the sediment yield estimates is caused by problems with the PSE methods, in particular their use of a non-linear discharge-turbidity model (Table 7). When the two data sets are processed in the same manner, my 2008-09 data always produce the higher sediment yield (Table 8). The measured discharge and sediment data between the two studies are consistent with each other. The 2011-12 data has a suspect peak on January 21st, 2012 that was discounted, as pointed out in Section 5.1. If this suspect peaks is removed, the PSE sediment yield drops 20% from 111,527,000 kg to 89,222,000 kg using the original PSE yield estimation methods. This is still more than three times the sediment

yield estimate from my 2008-09 season, which does not seem reasonable considering the smaller storm patterns and relative amounts of total discharge volume between the two seasons as pointed out in section 5.2.

7.4 Timing Characteristics

Turbidity peak timing correlates well with the timing of peak discharge and peak precipitation (Figures 18 and 19). The correlation of turbidity with discharge was weaker than with precipitation, possibly because turbidity is influenced primarily by precipitation and secondarily by discharge. Discharge is also primarily influenced by precipitation; however, a basin's response to a precipitation event is tied to a broader range of runoff processes that do not influence turbidity (e.g., vegetation, relief, antecedent soil water). As a result, hydrographs may only have one peak while the turbidity can peak several times to different magnitudes during the course of a storm (Figure 26). The hydrograph has smooth and even changes, and the overall shape is a result of the timing and intensity of precipitation spikes. Precipitation liberates sediment from the unvegetated toe and other exposed deposits near the stream, which flows directly into the stream channel. If discharge was only influenced by direct overland flow to the stream channel, the hydrograph would be similar to the plotted turbidity.

Even though I used the USGS South Pass Road data to investigate timing characteristics, I did examine periods of quality data in my data set. During the time frames of Feb 1-11, 2009 and Mar 18-30, 2009 the turbidity data collected at my station react to precipitation along with the discharge but the turbidity data more closely reflect the pattern of precipitation (Figure 26). Except for rare circumstances, each precipitation spike creates consequential turbidity spikes (Figures 10-14).

The pattern of precipitation has a significant impact on the time lag between turbidity and discharge peaks because both the shape of the hydrograph and the timing of turbidity peaks are influenced by precipitation patterns. Longer time lags occur when longer duration, low intensity storms cause a gradual rise in the hydrograph, but a relatively quick peak in turbidity. Turbidity can peak several times in one hydrograph but the highest turbidity peak will not consistently be the first peak, sometimes it will be the second or third peak. The time lag calculation between turbidity and discharge is significantly influenced by which turbidity peak is the highest.

The apparent correlation between precipitation and turbidity is so strong that discretion in interpreting should be exercised. It is important to note that it was not always possible to determine which peaks corresponded, so not every precipitation and turbidity peak was included in the correlation. As a result, the correlation is unquestionably subjective. Additionally, there were several turbidity peaks that had no apparent precipitation involvement. This could be explained by random mass wasting from the landslide toe, from unstable stream banks or from re-mobilization of settled material during a changing stage not necessarily caused by precipitation. Likewise, there were precipitation peaks that appeared to have no influence on turbidity. This could possibly be explained because the rain gauge is located at low elevation, near but not in the watershed, so that the recorded rainfall may not have occurred in the basin or possibly fell as snow at the higher elevations.

7.5 Magnitude Correlations

My attempt to use the USGS South Pass Road data to find relationships that could predict the magnitude of the turbidity response due to precipitation was inconclusive when

grouped together as a whole season. When the season was divided up into four two-month time brackets for the 2012-13 data by two weeks I improved the correlations. It makes sense that the same calendar time brackets would not apply to both seasons because of natural variations in weather patterns from year to year. The interesting aspect of this shift is that two months was still the optimal duration. I could make slight improvements in the correlations by varying the length of the brackets by shifting days from one bracket to the next. The correlations would again diminish with any adjustments greater than a week, which lends support to the two month durations.

Precipitation intensity does influence turbidity magnitudes but the correlation is influenced by two primary factors, the temporal proximity of storms and seasonal evolution of the basin hydrology. The correlation factors for the four time brackets in the 2012-13 have an overall decrease from the 2011-12 data, which could be explained by the difference in precipitation patterns. This is easily visible during the Oct-Nov bracket. In 2011-12, the storms were spaced out with simple, nearly stand-alone peaks. In 2012-13, the precipitation peaks were close together with variable peak magnitudes, therefore introducing significant variability in sediment erosion from peak to peak.

In both seasons, the turbidity magnitude correlations improve steadily over the season, with poor correlations at the beginning of both seasons and the best correlations at the end. One possible explanation for this pattern is that over the dry summer season, the sediment on the toe becomes dry and broken up by landslide motion without any means of removal, increasing the supply of easily erodible sediment. With the onset of the rainy season, the motion of the slide begins to accelerate. It is conceivable that pockets of the toe remain unsaturated while other pockets quickly become fully saturated. The relative

contribution of suspended sediment due to precipitation could be reflective of the level of saturation. This in turn might contribute to the variability in the measured sediment concentration during each storm. As the saturation with in the toe evens out during the first couple of months, the sediment release would become more consistent. As this occurs, the surface erosion resulting from precipitation becomes more predictable. This is a speculative explanation that I am not able to investigate with the data that I have available.

Another supporting explanation for the improved turbidity magnitude correlation over the season is that during the summer, streamflow diminishes to nearly unmeasurable levels, leaving behind deposits of landslide material. With the return of the rains, the streamflow increases and erodes these deposits, which would increase the variability of measured sediment concentration. The stream may change course several times within the streambed as the channel develops, diverting streamflow to or away from these pockets of left over sediment deposits, thus causing variability in the measured sediment concentration downstream. This process continues throughout the season but will be accentuated during the first couple of months of the rainy season.

7.6 Modeled Fall-Winter Sediment Yield

In spite of the limitations of discharge based sediment yield estimates, there are benefits from examining hydrologic variations from year to year. A well calibrated discharge model can provide continuous discharge that can easily be used to create sediment yield estimates for past years during which only precipitation data was recorded or to make future predictions.

I produced DHSVM hydrographs from 2009-2012 using Lawrence station MET data and applied my Discharge-TSS sediment yield estimation methods for those four years in order to compare sediment yield characteristics based on varying precipitation and discharge patterns from year to year. The linear model caused the predicted sediment yield to be influenced more by the magnitude of peak discharge rather than the total discharge volume over the complete season. Seasons with mild rainfall will produce low magnitude discharge peaks and because my model is linear the sediment yield will also be low. Seasons with one large storm will have a higher sediment yield than rainy seasons with mild consistent rain even if the total water volume is the same.

Improvements to the model should specifically address unequal matching of turbidity to discharge values during discharge evolution and the sediment hysteresis during multi-peak events. In the current model, the sediment flux is evenly distributed across the hydrograph when in fact the timing relationship of sediment flux with the hydrograph is more complex. The timing pattern is typically repetitive and predictable but can be influenced by outside hydrologic circumstances such as the soil saturation, the time elapsed since the previous storm, precipitation patterns and even the timing of freezing conditions.

8.0 Future Work

Future sediment yield estimates for the SCL should rely on Turbidity-TSS relationships from the USGS South Pass Road data or further developed Discharge-TSS relationships for Swift Creek. Turbidity-TSS modeling using data from the USGS gauges on the Sumas River is possibly the best solution for future TTS methods; however, one foreseeable problem of monitoring SCL derived suspended sediment in the Sumas River is the amount of deposition and dredging that occurs in the Oat Coles reach of Swift Creek.

Monitoring suspended sediment from Swift Creek directly sounds logical but previous attempts have determined that the creek is too temperamental to properly monitor using the TTS method. Efforts by PSE to gain more control of the flow and streambed morphology did not improve the quality of the data. Developing a Discharge-TSS relationship from the Sumas River is also plausible, but will require an improved understanding of both the storm timing effects on suspended sediment from the landslide and the hysteresis of sediment concentration.

Discharge modeling of the Swift Creek basin will continue to be important because of its difficult nature for stream monitoring. It would be beneficial to establish a rating curve for the more stable north sub-basin, along with continued discharge measurements downstream, to use for calibrating the DHSVM. By collecting discharge data for the main Swift Creek basin and the north sub-basin, researchers would be able to further examine the hydrologic influence of the landslide.

Other individual studies that would be beneficial to the overall picture could be quantifying the timing and sediment volume of mass wasting from the toe in relation to the timing and magnitude of precipitation. The morphology of the toe during the first couple of months of the rainy season could aid understanding of the turbidity fluctuations seen during these early season precipitation events. Using terrestrial laser scanning technology or photogrammetry to estimate changes in shape and volume of the toe during a major storm could provide a cross check of yield estimates for that time period.

9.0 CONCLUSION

This study provides an estimate of sediment yield during the winter season of 2008-09. The quality of the estimates provided in this thesis is poor because of incomplete data collection and the inherent problems with relating sediment to discharge. The significant differences between estimates derived from turbidity and discharge methods further diminish confidence in the accuracy of either type of estimate.

This study also provides a comparison of sediment yield estimates and methods between my 2008-09 study and PSE's 2011-12 study. My study derived sediment yield estimates from linear Turbidity-TSS and Discharge-TSS relationships. PSE's estimate was derived through an indirect Turbidity-Discharge polynomial relationship and a Turbidity-TSS linear relationship. The PSE sediment yield estimate was more than four times the predicted yield from my study. The PSE measured discharge and TSS data are close in magnitude to my measured data, however, the predicted PSE turbidity and TSS data were an order of magnitude larger than the measured data. My predictive model produced results similar to the measured data of both studies. When PSE's prediction methods were applied to my data, the resulting TSS were also an order of magnitude higher than measured values, indicating a problem with their estimation process.

There are significant uncertainties in both studies because of noisy turbidity data, sparse TSS and discharge (for 2008-09 season) measurements, instrument failures and other measurement limitations. These uncertainties make it difficult to determine which estimate yield to give the most confidence. There is, however, some positive support for my estimate methods due to the similarity of my predicted TSS to the measured TSS of both studies. I make this case because of how TSS is controlled by precipitation and discharge. The two

seasons have comparable measured values of precipitation and discharge. It would be reasonable to assume that if PSE's measured discharge and precipitation maximum were similar to mine, there would also be similar TSS measurements, which was the case. The maximum TSS measurements that occurred during the largest storm of my season likely represent the upper boundary for concentration for that season, as multiple samples were taken throughout the storm surrounding the peak. All the other samples from smaller storms during my season had much lower concentrations as would be expected. Therefore, the correlation between precipitation, discharge and sediment concentration would suggest that PSE's maximum measured TSS is also representative of the seasonal high, which my methods support when used with PSE data. It stands to reason that PSE's methods should also have predicted TSS values that were similar to measured values, but this was not the case.

From my study, it appears that hydrology was useful in understanding the nature of sediment flux in the Swift Creek basin. The timing between turbidity, discharge and precipitation using the USGS Sumas River South Pass Road turbidity and discharge data along with the Lawrence station precipitation reveals a relatively consistent and predictable pattern between hydrology and sediment flux. The magnitudes of sediment flux, however, are less predictable by hydrology with simple linear models, but there is a trend of increasing predictability over the course of a season as the landslide sediment and hydrologic conditions stabilize.

10.0 REFERENCES

Bayer, T.M., 2006, The Nature and Transport of the Fine-Grained Component of Swift Creek Landslide, Northwest Washington, MS Thesis, Western Washington University

Bayer, T. M. and Linneman, S., 2010, The nature and transport of the fine-grained component of Swift Creek Landslide, Northwest Washington. Earth Surf. Process. Landforms, 36: 624–640. doi: 10.1002/esp.2081

Benkhaled, A. and Remini, B., 2003. Variabilité temporelle de la concentration en sédiments et phénomène d'hystérésis dans le bassin de l'Oued Wahrane (Algérie) / Temporal variability of sediment concentration and hysteresis phenomena in the Wadi Wahrane basin, Algeria. Hydrological Sciences Journal/Journal des Sciences Hydrologiques, 48(2): 243-255.

Bernstein, D., J. Dunnigan, T. Hesterberg, R. Brown, J.A.L. Velasco, R. Barrera, J. Hoskins, and A. Gibbs, 2013, Health Risk of Chrysotile Revisted, Critical Reviews in Toxicology, 43(2): 154-183, 2013 Healthcare USA, Inc. DOI: 10.3109/10408444.2012.756454

Brasington, J. and Richards, K., 2000, Turbidity and suspended sediment dynamics in small catchments in the Nepal Middle Hills. Hydrological Processes, 14(14): 2559-2574.

Brayfield, B.M., 2013, Modeling Slope Failure in the Jones Creek Watershed, Acme, Washington. Master of Science Thesis, Western Washington University.

Chappell, N.A., Douglas, I., Hanapi, J.M. and Tych, W., 2004. Sources of suspended sediment within a tropical catchment recovering from selective logging. Hydrological Processes, 18(4): 685-701.

Chennault. J. 2004, Modeling the contribution of glacial meltwater to streamflow in Thunder Creek, North Cascades National Park, Washington. Master of Science Thesis, Western Washington University.

Cyphert, J., A. Nyska, R. Mahony, M. Schladweiler, U. Kodavanti, S. Gavett, 2012, Sumas Mountain Chrysotile Induces Greater Lung Fibrosis in Fischer 344 Rats than Libby Amphibole, El Dorado Tremolite, and Ontario Ferroactinolite, Oxford University Press, Toxicological Sciences, TOXSCI-12-0412.R1

Dickerson, S.E., 2010, Modeling the Effects of Climate Change Forecasts on Streamflow in the Nooksack River Basin. Master of Science Thesis, Western Washington University.

Donnell, C., 2007, Quantifying the glacial meltwater component of Streamflow in the Middle Fork Nooksack River, Whatcom County WA using a distributed hydrology model. Master of Science Thesis, Western Washington University.

Doten, C.O., and D.P. Lettenmaier, 2004, Prediction of Sediment Erosion and Transport with the Distributed Hydrology-Soil-Vegetation Model, Water Resources Series Technical Report No. 178.

Doten, C.O., L.C. Bowling, J.S. Lanini, E.P. Maurer, and D.P. Lettenmaier, 2006, A Spatially Distributed Model for the Dynamic Prediction of Sediment Erosion and Transport in Mountainous Forested Watersheds, Water Resources Series Technical Report No. 178.

Dragovich, J.D., D.K. Norman, R.A. Haugerud, and P.T. Pringle, 1997, Washington division of Geology and Earth Resources Open File Report 97-2.

Fenton, C., 2006, Turbidity and Suspended Sediment Yields Freshwater Creek and Elk River Operations Report, Salmon Forever/Watershed Watch, HY 2005, Redwood Community Action Agency Humboldt Bay Water Quality Improvement Program, Contract # SWRCB 03-212-551-0

Fubini B, Arean C. O. 1999. Chemical aspects of the toxicity of inhaled mineral dusts. Chem. Soc. Rev. 28: 373-381

Gulumian M. 2000. The ability of mineral dusts and fibers to initiate lipid peroxidation. Part ii: Relationship to different particle induced pathological effects. Redox Rep. 5: 325-351

Hanell, C.R., 2011, Groundwater Response to Precipitation Events, Kalaloch, Olympic Peninsula, Washington. Master of Science Thesis, Western Washington University.

Holmes, E.P., J. Wilson, H. Schreier, and L.M. Lavkulich, 2012, Processes affecting surface and chemical Properties of Chrysotile: Implications for reclamation of Asbestos in the Natural Environment, Canadian Journal of Soil Science, Vol. 92, No. 1, Jan 2012.

Keim, R.R. and A.E. Skaugset, 2003, Modelling effects of forest canopies on slope stability, Hydrological Processes, v. 17, p. 1457-1467

Kelleher, K. 2006, Streamflow calibration of two sub-basins in the Lake Whatcom Watershed, Washington using a distributed hydrology model. MS Thesis, Western Washington University.

Kerr Wood Leidal Associates Ltd. Swift Creek Management Plan, 2005, Report.

Krause P, Boyle DP, Bäse F. 2005. Comparison of different efficiency criteria for hydrological model assessment. Advances in Geosciences 5: 89-97.

Kunkle, S.H. and Comer, G.H., 1971. Estimating suspended sediment concentrations in streams by turbidity measurements. Journal of Soil and Water Conservation, 26(1): 18-20.

Lewis, J., 1996. Turbidity-controlled suspended sediment sampling for runoff-event load estimation. Water Resources Research, 32(7): 2299-2310.

Lewis, J., 2002, Estimation of Suspended Sediment Flux in Streams Using Continuous Turbidity and Flow Data Coupled with Laboratory Concentrations, Turbidity and other sediment surrogates workshop, 30 April – 02 May 2002, Reno, Nevada. 3 p.

Lewis, J. and Eads, R., 1996. Turbidity-controlled suspended sediment sampling, Watershed Management Council Networker.

Lewis, J., R. Eads, 2008, Implementation Guide for Turbidity Threshold Sampling: Principles, Procedures, and Analysis, General Technical Report PSW-GTR-212. Arcata, CA: U.S. Department of Agriculture, Forest Service, Pacific Southwest Research Station.

Linneman, S.R., D.L. Clark, 2006, Western Washington University Landscape Observatory, http://www.wwu.edu/landscapeobservatory/index.shtml

Linneman, S.R., P. Pittman, 2009, The Source of Asbestiform Chrysotile at Swift Creek WA: Geology, Mineralogy and Sediment Transport, Portland GSA Annual Meeting, 18-21 October 2009, Session No. 274.

Manka, P., 2005. Suspended sediment yeilds in tributaries of Elk River, Humboldt County, California. Master of Science Thesis, Humboldt State University, Arcata.

Magirl, C.S., Curran, C.A., Czuba, C.R., Cox, S.E., Sumioka, S., Miller, D., Czuba, J.A., Marineau, M., and Kahle, S., 2011, Assessment of transport and deposition of asbestos-rich sediment along Swift Creek and the Sumas River, Whatcom County, Washington—Year-One Status Report: presented to the Environmental Protection Agency, Region X, Seattle, WA, September 29, 2011. Matthews, R., M. Hilles, J. Vandersypen, R. Mitchell and G. Matthews, 2007, Lake Whatcom Monitoring Report 2005-2006.

McKenzie-Johnson, A.S., 2004, Kinematics of the Swift Creek Landslide, Northwest Washington, MS Thesis, Western Washington University.

Meadows, M.W. 2009, Using in situ Turbidity to Estimate Sediment Loads in Forested Headwater Streams: A Top-down versus Bottom-up Approach. Master of Science Thesis, Oregon State University.

Melious, J.O., 2013, The Emerging Legal Problem of Naturally Occurring Asbestos and Washington State's Swift Creek Conundrum, Seattle Journal of Environmental Law, http://www.sjel.org/vol2/naturally-occurring-asbestos.html, 19 March 2012.

Miller, W. J., 1931, The landslide at Point Firmin, California, Science Monthly, 32, 464–469.

Nash JE, Sutcliffe JV. 1970. River flow forecasting through conceptual models; Part I, A discussion of principles. Journal of Hydrology 10(3): 282–290.

Oze C, Solt K. 2010. Biodurability of chyrostile and tremolite asbestos in simulated lung and gastric fluids. Am. Miner. 95: 825-831

Pacific Surveying & Engineering, Inc. (PSE) 2012, Sediment Basin Suspended Sediment Analysis, Supplement to the SCSMAP Phase 1 Conceptual Design, Prepared for Whatcom County Public Works, November 15, 2012

Petley, D.N., R.J. Allison, 1997, The Mechanics of Deep-Seated Landslides., Earth surface Processes and Landforms, Vol 22, p 747-758.

Pfannkuche, J. and Schmidt, A., 2003. Determination of suspended particulate matter concentration from turbidity measurements: particle size effects and calibration procedures. Hydrological Processes, 17(10): 1951-1963.

Radbruch-Hall, D. H., 1978, Gravitational creep of rock masses on slopes, in Voight, B. (Ed.), Rockslides and Avalanches, Elsevier,Amsterdam, 607–657.

Rantz, S. E., 1982, Measurement and computation of streamflow, volume 1: Measurement of stage and discharge: U.S. Geological Survey Water-Supply Paper 2175, 80 p.

Smith, B.P., Naden, P.S., Leeks, G.J.L. and Wass, P.D., 2003. The influence of storm events on fine sediment transport, erosion and deposition within a reach of the River Swale, Yorkshire, UK. The Science of the Total Environment, 314-316: 451-474.

Sun, H., Cornish, P.S. and Daniell, T.M., 2001. Turbidity-based erosion estimation in a catchment in South Australia. Journal of Hydrology, 253(1): 227-238.

Swift Creek Sediment Management Action Plan (SCSMAP), 2012, Whatcom County Public Works on behalf of Whatcom County Flood Control Zone District.

United States Department of Agriculture (USDA), Natural Resources Conservation (NRCS). 2001. State Soil Geographic (STATSGO) Data Base: Data Use Information. http://www.nrcs.usda.gov/technical/techtools/statsgo_db.pdf

United States Environmental Protection Agency (EPA), 2011, Sumas Mountain Asbestos Update – October 2011, Swift Creek and Sumas River Whatcom County Flooding Fact Sheet for Residents, October 2011.

United States Geological Society (USGS), 2013, Turbidity – Units of Measurement, Oregon Water Science Center, January 4, 2013, http://or.water.usgs.gov/grapher/fnu.html, May 16, 2014.

Vanshaar, J., and D.P. Lettenmaier, 2001, Effects of Landcover Change on the Hydrologic Response of Pacific Northwest Forested Watersheds. Water Resources Series Technical Report No. 165.

Vanshaar, J., I. Haddeland, and D.P. Lettenmaier, 2002, Effects of land-cover changes on the hydrological response of interior Columbia River basin forested catchments: Hydrological Process, v. 16, p. 2499-2520.

Washington State Department of Health, 2010, Sumas Mountain/Swift Creek Asbestos Cluster Investigation, N. West and G. Patrick, Environmental Epidemiology, Division of Environmental Health, DOH 334-224 February 2010.

Western Regional Climate Center, 2013, Washington Climate Summaries, http://www.wrcc.dri.edu/summary/climsmwa.html, 3 July, 2013.

Wigmosta, M.S., Vail, L.W., and D.P. Lettenmaier, 1994, A distributed hydrology-vegetation model for complex terrain. Water Resources Research, 30(6), 1665-1679.

Young, K. B., 1950, A comparative study of mean-section and mid-section methods for computation of discharge measurements: U.S. Geol. Survey open-file report, 52 p.

11.0 TABLES

Table 1: List of Swift Creek Investigations after SCSMAP.

Year	Swift Creek Watershed and Landslide Investigations
1990	Landau Associates Inc. 1990. Swift Creek Investigation Report, Whatcom County, Washington. Report prepared for Whatcom County Engineering Department, Bellingham, Washington.
1998	GeoEngineers, Inc. 1998. Geotechnical Engineering Services, Stream Management Plan for Swift Creek, Whatcom County, Washington.
2004	McKenzie-Johnson, Kinematics of the Swift Creek Landslide, Northwest Washington, MS Thesis, Western Washington University
2005	BGC Engineering, Inc. 2005. Swift Creek Landslide Study, Whatcom County, Washington.
2005	Bayer, The Nature and Transport of the Fine-Grained Component of Swift Creek Landslide, Northwest Washington, MS Thesis, Western Washington University
2008	Kerr Wood Leidal Associates, LTD. 2008. Swift Creek Background and Management Alternatives.
2008	Whatcom County Public Works, Washington State Department of Ecology, U.S. Environmental Protection Agency. 2008. Swift Creek Short to Mid-Term Sediment Management Alternatives Assessment: Cooperative Internal Staff Report. Whatcom County, Washington.
2009	Bennett Engineering, LLC. 2009. Groundwater Investigation Report, Swift Creek Vicinity Between Goodwin Road and Oat Coles Road. Whatcom County, Washington.
2010	Pacific Surveying & Engineering, Inc. 2010. Sumas Mountain Naturally Occurring Asbestos Interim Alternatives Analysis. Whatcom County, Washington.

Table 2: List of Swift Creek History after SCSMAP.

Year	Swift Creek History
1940s	Swift Creek landslide is reactivated; first reports to Whatcom County of channel filling with sediment
1940s - 1971	Soil Conservation Service (SCS) helps with sediment management
1960s - 1970s	Whatcom County, SCS and U.S. Army Corps of Engineers begin working together to manage Swift Creek
1971	Rain-on-snow event causes debris dam outbreak below the landslide, delivering an estimated 150,000 cubic yards of material downstream in debris flow event
1971	U.S. Army Corps of Engineers dredges portions of the main channel and uses dredged material to construct levees along creek banks to reduce future flood risk
1970s - 2006	Whatcom County routinely conducts channel maintenance dredging, primarily below Goodwin Road, to maintain use of area bridges and roadways; sediment upstream of Goodwin Road managed privately
1998, 2005	"Big dig" channel dredging to restore channel bed elevations to pre-debris flow levels
2005-2007	EPA conducts a health risk assessment and concludes that "significant" asbestosrelated health risks are associated with Swift Creek sediment; Whatcom County is advised that new sediment management strategies will be necessary
2007	Whatcom County requests federal and state assistance in resolving management dilemma stemming from EPA findings
2007	EPA stabilizes Swift Creek sediment stockpiles with tackifier
2007 - Present	Whatcom County continues to balance health risks with sediment management need

Table 3: List of the regulatory framework governing the Swift Creek watershed after SCSMAP.

Federal	Washington State	Whatcom County
• Clean Water Act -Section 401 -Section 402 -Section 404 • National Flood Insurance Act (NFIP)/Flood Disaster Protection Act • Coastal Zone Management Act • National Environmental Policy Act • Comprehensive Environmental Response Compensation and Liability Act	• Floodplain Statutes -Flood Control by Counties -Floodplain Management • Water Pollution Control Act • Shorline Management Act • Washington Hydraulic Code • State Environmental Policy • Model Toxics Control Act • Washington Sediment Management Standards	• Comprehensive Plan • Zoning Ordinance • Shoreline Management Program • Flood Damage Prevention Ordinance • Critical Areas Ordinance • SEPA Ordinance

Table 4: Turbidity and discharge peak time analysis, in hours, using data from the USGS South Pass gauge, 2011-12. Discharge peaks lag behind turbidity peaks.

Storm	Date	t_{Tp}	t_{qp}	T_{LP}	Notes
1	Apr 27 - May 5, 11	6	15	9	Example of perfect conditions
2	May 2 - May 5, 11	5	11	6	Example of perfect conditions
3	May 5 - May 10, 11	57	62	5	52 hr lead in with small precip causing turbity peaks and hydrograph changes
4	Dec 26 - Jan 2, 11	49	61	12	Multi peak turbidity, Has a really weird peak peak
5	Jan 2 - 13, 11	54	63	9	Multipeak Turbidity, Symmetrical Hydrograph
6	Jan 13 - 20, 12	27	30	3	Interesting, many turb peaks after response hydrograph
7	Jan 20 - 24, 12	22	35	13	Example of perfect conditions
8	Jan 24 - 28, 12	23	30	7	Rounded & Symmetrical hydrograph on falling limb of peak 4, 2 Turb peaks
9	Jan 28 - 31, 12	31	32	1	Extensive gap in turbidity data
10	Feb 1 - 16, 12	5	15	10	Happened Quick on falling limb of peak 6, missing turbidity
11	Feb 16 - 20, 12	37	74	37	Strong initial T peak, several small ones on the rising limb, Longer rising limb
12	Feb 20 - 24, 12	21	31	10	Extensive gap in turbidity, symmetrical hydrograph
13	Feb 24 - Mar 2, 12	20	39	19	Hydrograph fell faster than it rose
14	Mar 2 - 9, 12	58	69	11	Several small preceding turbity peaks before main peak
15	Mar 9 - 15, 12	19	35	16	Dual turbity peak, equal magnitude
16	Mar 15 - 26, 12	15	30	15	Noisy turbity, could be a false peak
17	Mar 26 - 31, 12	6	35	29	Rounded Hydrograph, dual peak turb
18	Mar 31 - Apr 3, 12	20	27	7	Oddly solitary turb peak with a predecessor
19	Apr 3 - 6, 12	4	12	8	Dual peak turb

t_{Tp} = time of peak turbidity

t_{qp} = time of peqak discharge

T_{LP} = peak lag (t_{qp} -t_{Tp})

Min	Max	Ave	Mode	St Dev
1.0	37.0	11.9	9.0	8.7

Table 5: Turbidity and Precipitation peak time analysis from the USGS South Pass gauge, 2011-12. All time relationships are in hours.

Storm	Date	t_{Tp}	t_{wp}	T_{LP}	Notes
1	Apr 27 - May 5, 11	6	2	-4	
		9	5	-4	
		28	18	-10	
		46	44	-2	
		69	68	-1	
2	May 2 - May 5, 11	7	2	-5	
		13	6	-7	
3	May 5 - May 10, 11	5	5	0	
		25	24	-1	
		44	43	-1	
		57	54	-3	
4	Dec 26 - Jan 2, 11	30	25	-5	
		36	32	-4	
		49	45	-4	
		56	52	-4	
5	Jan 2 - 13, 11	11	5	-6	
		26	21	-5	
		46	39	-7	
		55	51	-4	
6	Jan 13 - 20, 12	27	17	-10	
		31	26	-5	
7	Jan 20 - 24, 12	22	18	-4	Strong initial precip peak but no reaction in Turb
		54	50	-4	
		57	53	-4	
8	Jan 24 - 28, 12	1	1	0	Bi-modal Turb, 2nd turb peak is largest, 1st precip is largest
		9	4	-5	
		12	8	-4	
		26	22	-4	
		34	30	-4	
		38	35	-3	
9	Jan 28 - 31, 12	7	2	-5	Huge gap in Turbidity
		11	6	-5	

t_{Tp} = Time to peak of the turbidity response.

t_{wp} = Time to peak of precipitation

T_{LP} = Peak lag (t_{wp} -t_{Tp})

Table 5 Continued

Storm	Date	t_{Tp}	t_{wp}	T_{LP}	Notes
10	Feb 1 - 16, 12	6	5	-1	Small gap in Turb at the peak
		41	37	-4	
		77	74	-3	
		23	20	-3	
11	Feb 16 - 20, 12	13	7	-6	
		42	38	-4	
		61	59	-2	
		73	70	-3	
12	Feb 20 - 24, 12	27	21	-6	Big gap in Turbidity, symmetrical hydrograph
		36	32	-4	
13	Feb 24 - Mar 2, 12	13	10	-3	Turb doesn't react enough to all the precip peaks
		27	24	-3	
14	Mar 2 - 9, 12	37	31	-6	
		46	43	-3	
		66	59	-7	
		66	63	-3	
		71	69	-2	
15	Mar 9 - 15, 12	5	2	-3	
		19	14	-5	
		29	26	-3	
16	Mar 15 - 26, 12	6	1	-5	
		11	4	-7	
		18	13	-5	
		26	21	-5	
		34	30	-4	
17	Mar 26 - 31, 12	50	44	-6	
		85	82	-3	
		99	95	-4	
		111	106	-5	
18	Mar 31 - Apr 3, 12	3	1	-2	
		10	6	-4	
		18	14	-4	
		22	18	-4	
		27	20	-7	
19	Apr 3 - 6, 12	9	2	-7	
		17	12	-5	

t_{Tp} = Time to peak of the turbidity response.

t_{wp} = Time to peak of precipitation

T_{LP} = Peak lag (t_{wp} -t_{Tp})

min	max	average	mode	st dev
-10.0	0.0	-4.2	-4.0	1.9

Table 6: Discharge and precipitation maxima and percentages of seasonal totals

Storm Dates	Peak Discharge (m^3/s)	Total Discharge (m^3)	Peak Precip (cm/hr)	Total Precip (cm)	% Total Discharge	% Total Precip
November 1-17, 2008	4.2	1,439,244	0.76	22.2	41%	55%
January 6-12, 2009	6.6	1,532,471	0.58	14.9	44%	40%
November 22-30, 2011	2.7	319,427	1.07	6.6	8%	12%
January 18-23, 2012*	4.2	481,159	0.25	2.4	12%	4.5%
March 9-12, 2012	3.3	352,954	0.28	2.9	9%	5.5%

* Discharge peak was determined to be a false peak.

Table 7: Precipitation (mm) from PSE and Clement

	PSE	Clement
Max	10.7	5.8
Min	0	0
Ave	0.124	0.121

Discharge (m^3/s) from PSE and Clement

	PSE	Clement
Max	4.2	6.6
Min	0	1
Ave	0.28	0.25

Measured TSS (mg/L) from PSE and Clement

	PSE	Clement
Max	13,500	20,686
Min	1	77
Ave	2,798	2,438

Comparison of hourly yield (kg) between PSE and Clement

		PSE	PSE data Clement Model	Clement	Clement data PSE Model
Modeled TSS (mg/L)	Max	310,564	14,183	22,065	608,576
	Min	0	663	776	71
	Ave	4,273	1,562	1,617	7,541

Table 8: DHSVM discharge and sediment yield statistics from multiple years. Sediment Yield was calculated using the Discharge-TSS relationship from the Goodwin Road Bridge data.

Beginning in Oct 2008

Water Year	(m^3)	% of 2009	Discharge ($m^{3/s}$)				% of 2009
Oct-Mar	Total Yield	Yield	min	max	ave	Total (m^3)	max discharge
2009	21,797	100%	0.04	6.6	0.28	5,140,278	100%
2010	12,691	58%	0.03	3.45	0.34	5,544,692	52%
2011	16,550	76%	0.04	3.85	0.4	5,349,735	58%
2012	7,753	36%	0.03	2.63	0.28	3,924,093	40%

Total Yield Average	Total Discharge Average
14,698	4,989,700
Standard Deviation	Standard Deviation
5,947	729,345

12.0 FIGURES

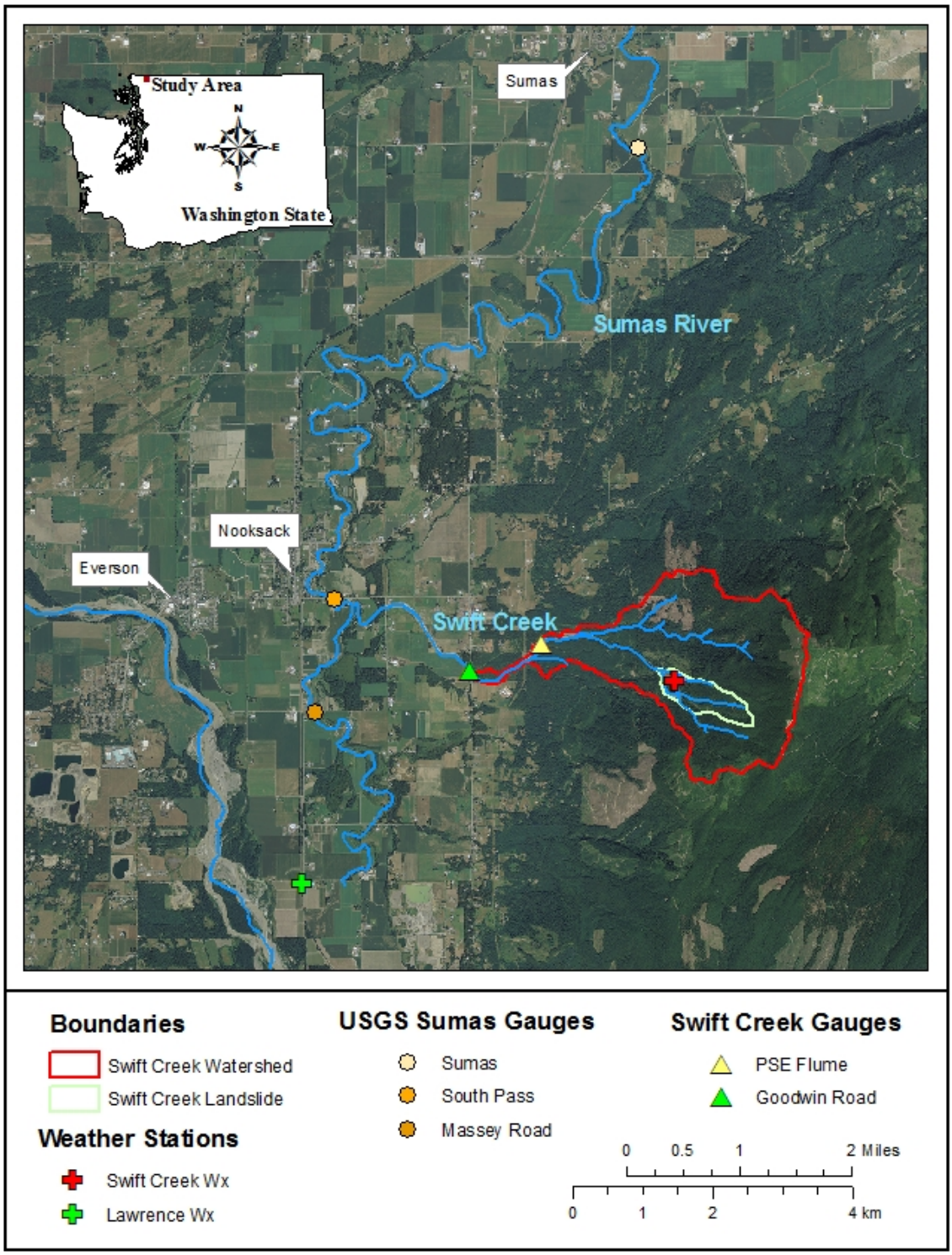

Figure 1: Swift Creek location map. The Swift Creek watershed is shown in red just east of Everson on Sumas Mountain. Two weather stations are in close proximity to Swift Creek shown by the crosses.

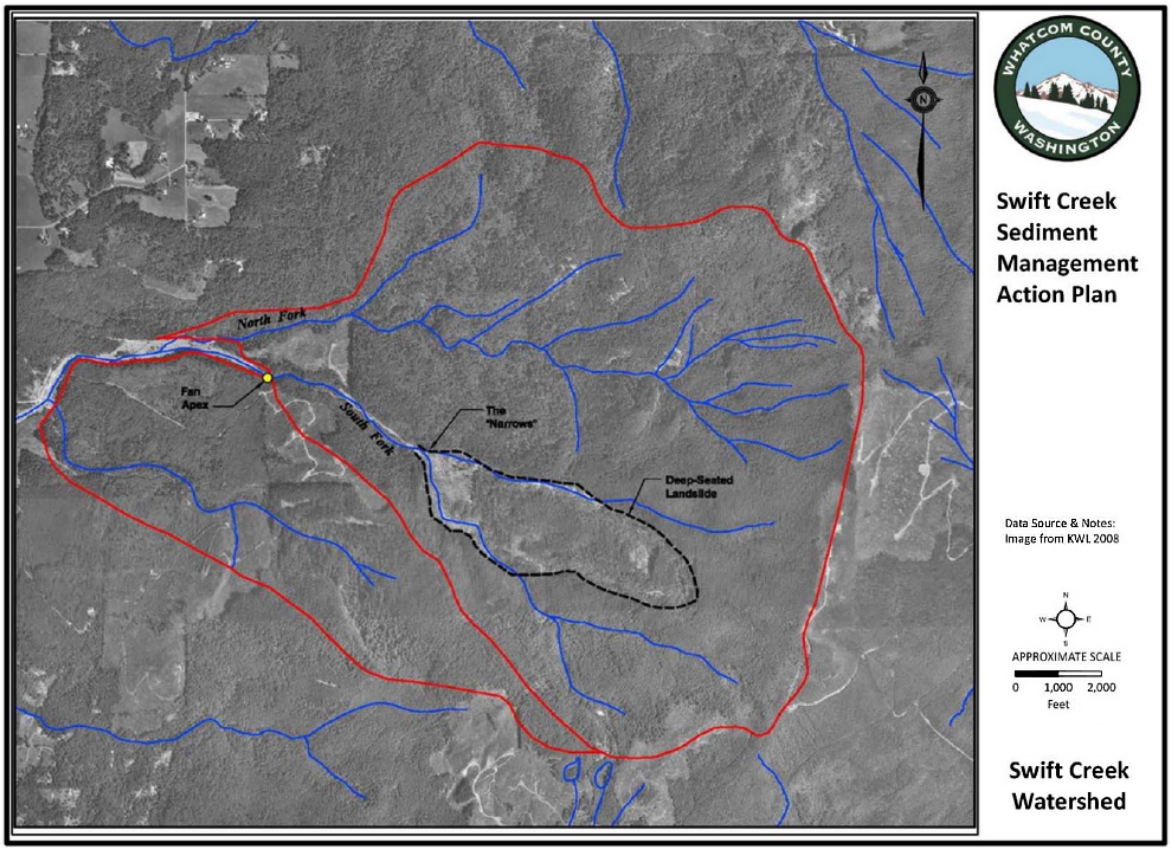

Figure 2: Upper watershed boundary (after SCSMAP, 2012). The lower watershed extends into the upper watershed up to the fan apex.

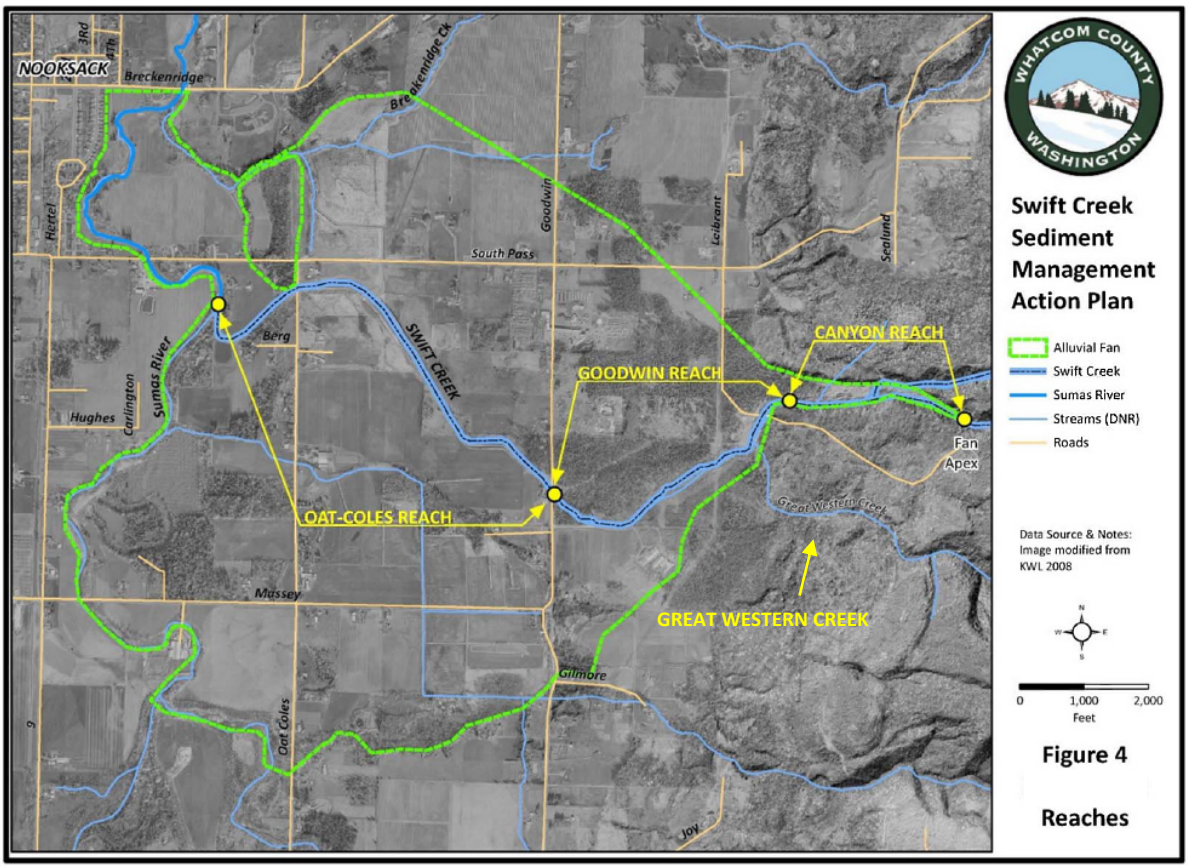

Figure 3: Swift Creek lower watershed nomenclature (after SCSMAP, 2012).

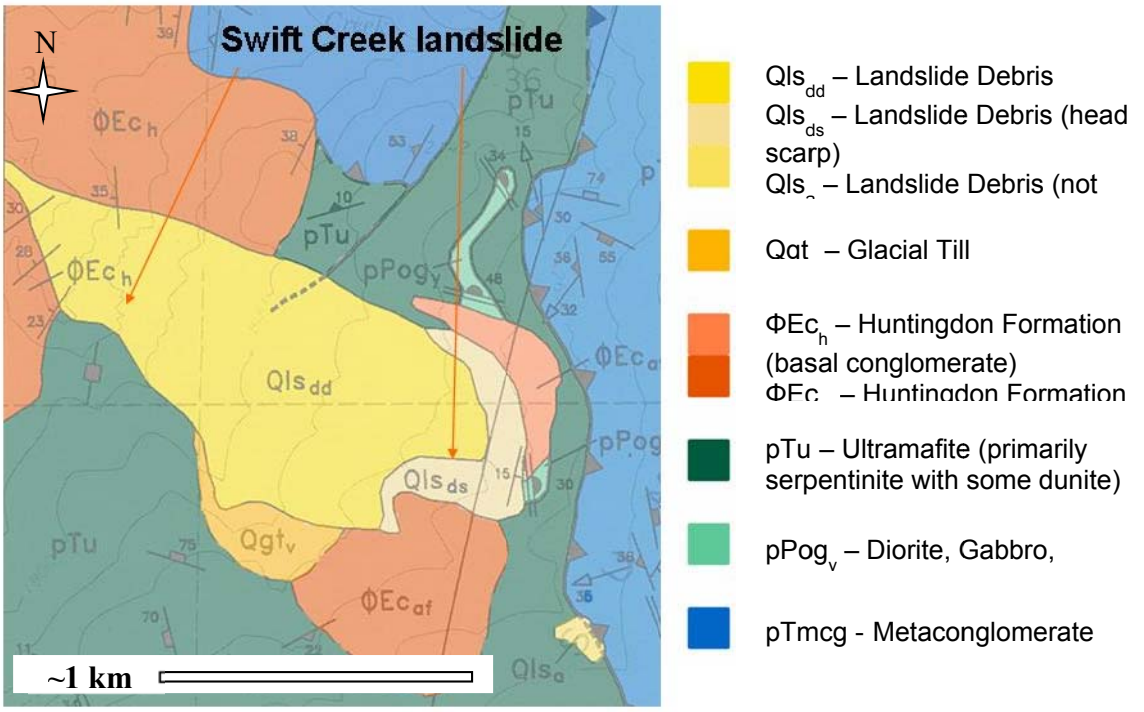

Figure 4: Geologic map of Swift Creek Landslide and adjoining areas (after Dragovich et al., 1997).

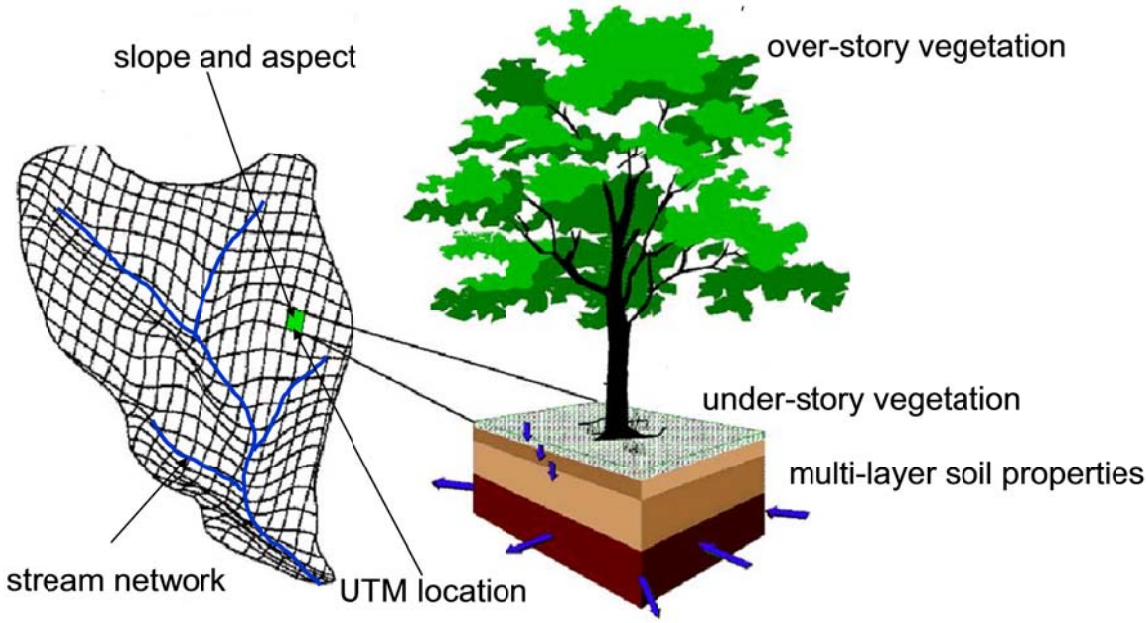

Figure 5: Simplified DHSVM hydraulic diagram depicting the physical characteristics and interaction between grid cells in DHSVM (Wigmosta et al., 1994).

Figure 6: Stream gauge equipment setup for Turbidity Threshold Sampling at the Goodwin Road bridge, including a hinging boom mount for a turbidity sensor and vacuum tube suspended 2m from the bridge, a stilling well mounted on north side of stream fixed the bridge Turbidity data logger and ISCO water sampler are contained in the box mounted safely to the guard rail. View to northeast, stream flow is to the lower left.

Figure 7: Stream gauge controls. Turbidity data logger, 12 volt battery and ISCO water sampling instruments.

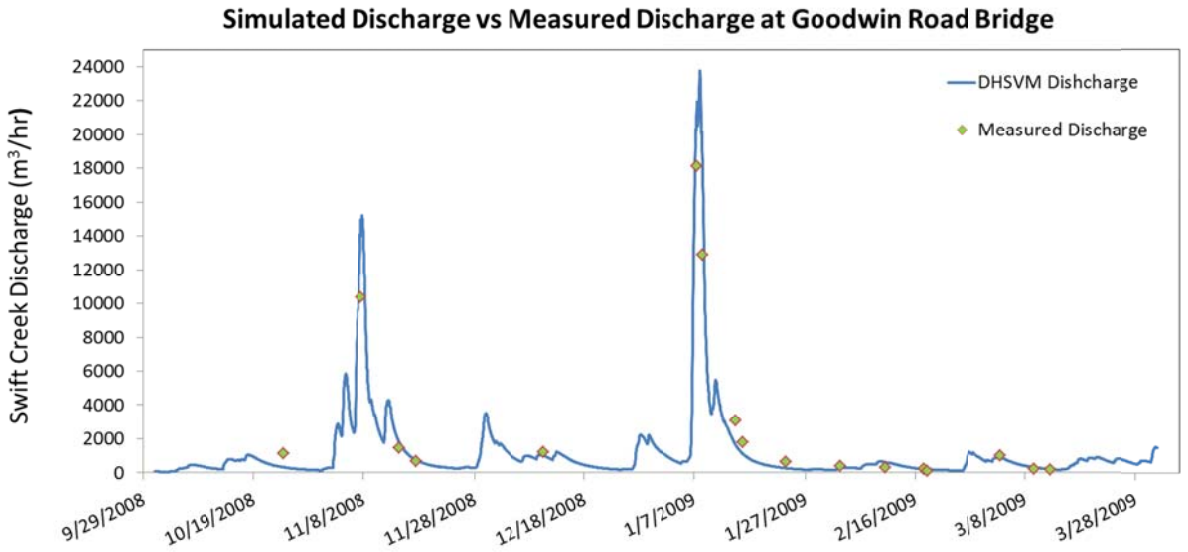

Figure 8: 2008-09 discharge plot of measured discharge with modeled DHSVM hydrograph at the Goodwin Road Bridge.

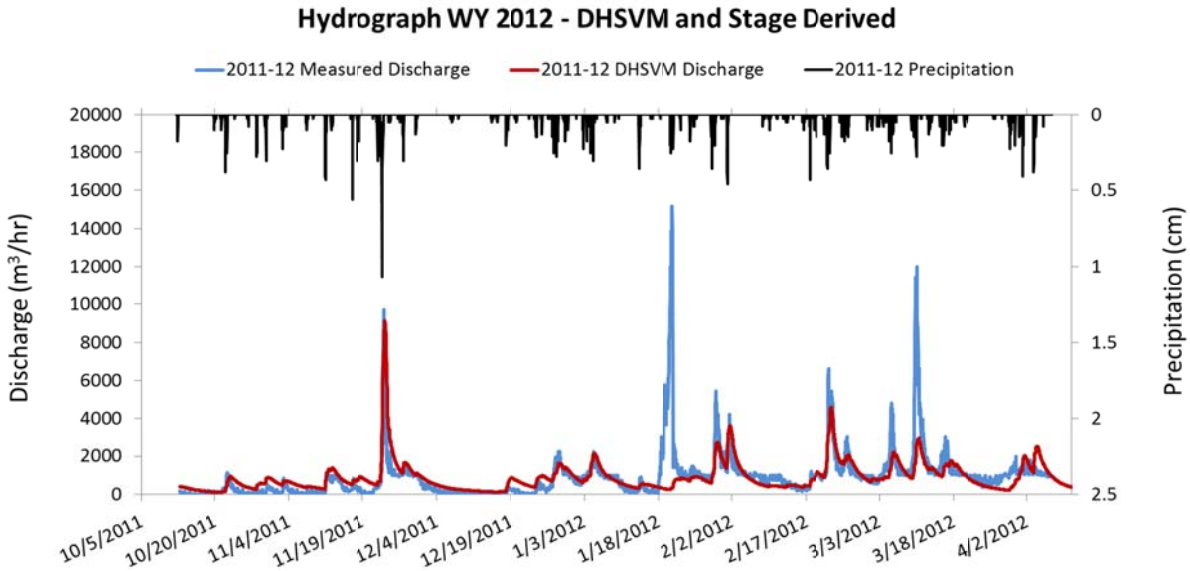

Figure 9: Modeled and measured discharge and precipitation from the PSE station to validate calibrated DHSVM model.

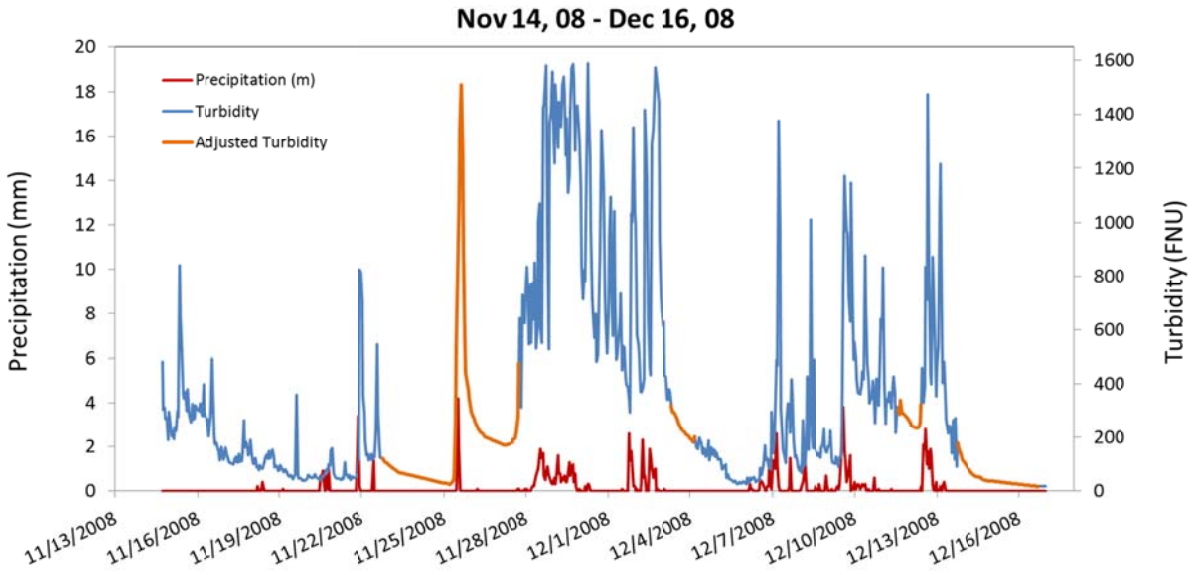

Figure 10: Turbidity and precipitation from 14 Nov, 08 - 16 Dec, 08. Turbidity from the Goodwin Road gauge, precipitation from Lawrence station.

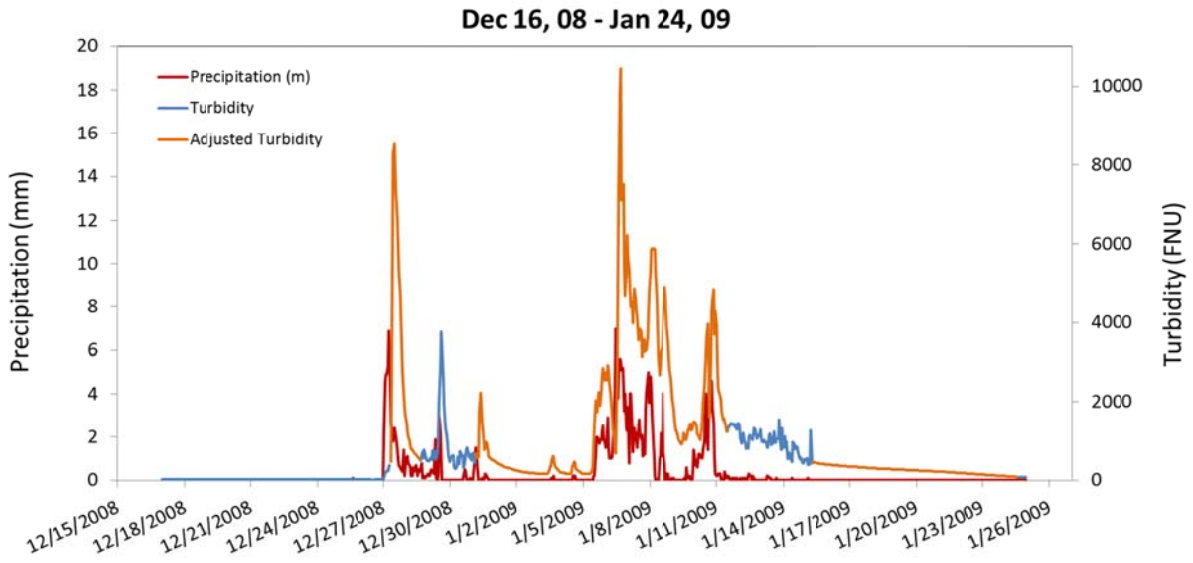

Figure 11: Turbidity and precipitation from 16 Dec, 08 – 24 Jan, 09. Turbidity from the Goodwin Road gauge, precipitation from Lawrence station.

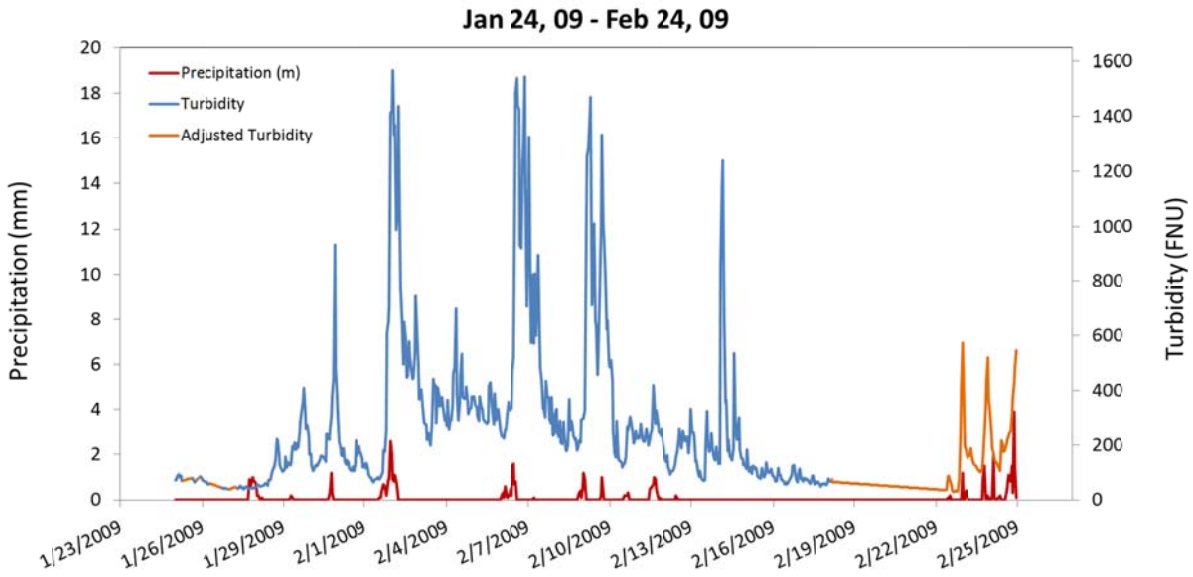

Figure 12: Turbidity and precipitation from 24 Jan, 09 – 24 Feb, 09. Turbidity from the Goodwin Road gauge, precipitation from Lawrence station.

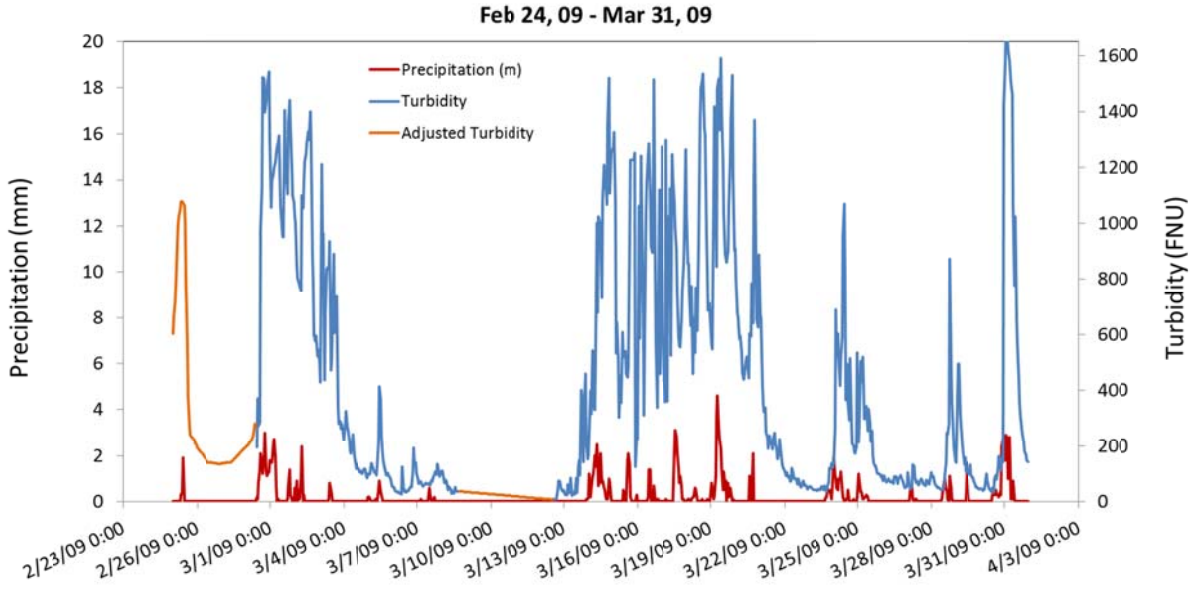

Figure 13: Turbidity and precipitation from 24 Feb, 09 – 31 Mar, 09. Turbidity from the Goodwin Road gauge, precipitation from Lawrence station.

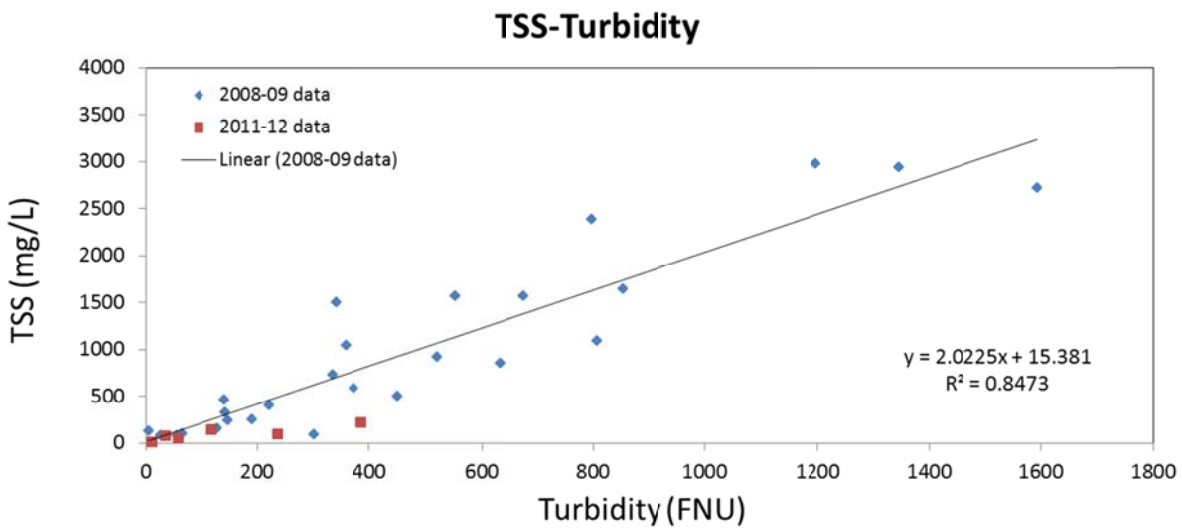

Figure 14: My 2008-09 Turbidity-TSS correlation using measured TSS and measured turbidity from the Goodwin Road Bridge. The small sample set from the 2012 study is visible in the plot but not included in the linear regression.

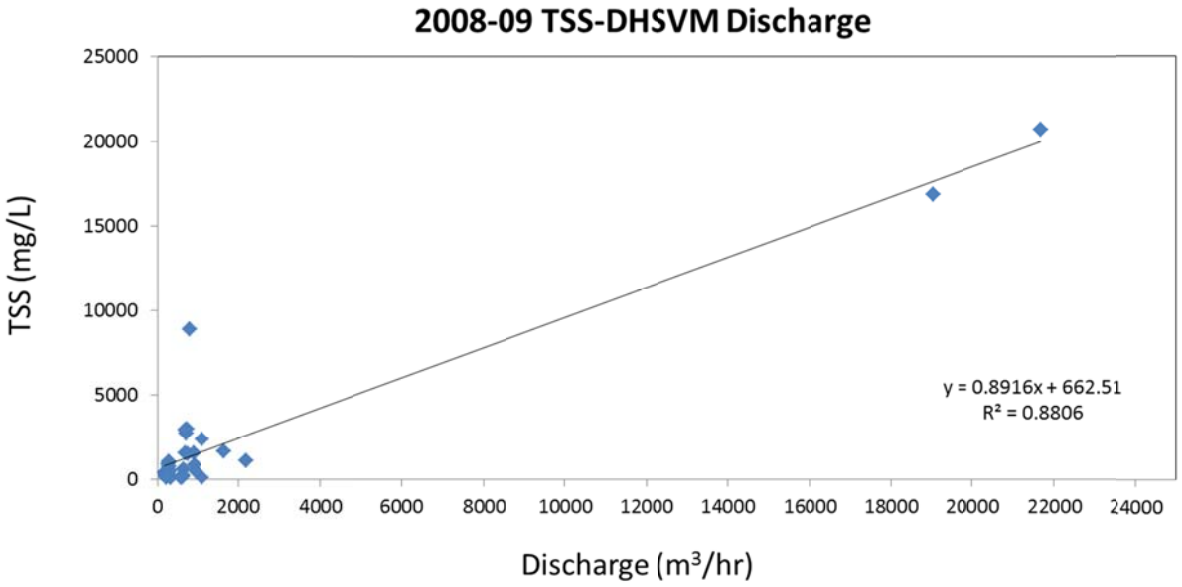

Figure 15: My 2008-09 Discharge-TSS correlation using the DHSVM discharge and measured TSS from the Goodwin Road Bridge.

Figure 16: PSE gauging station (from PSE, 2012). View to southeast, stream flow is to the right.

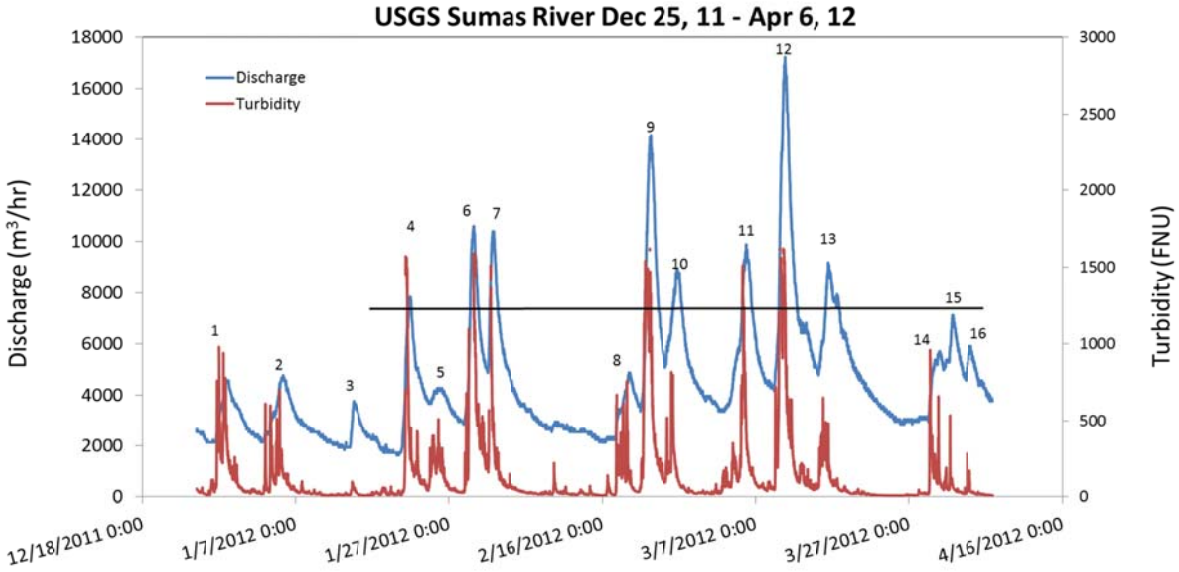

Figure 17: 2011-12 Sumas River discharge and turbidity data from the USGS South Pass Road gauge. Line struck to aid comparison of peak magnitude between peaks 4-13.

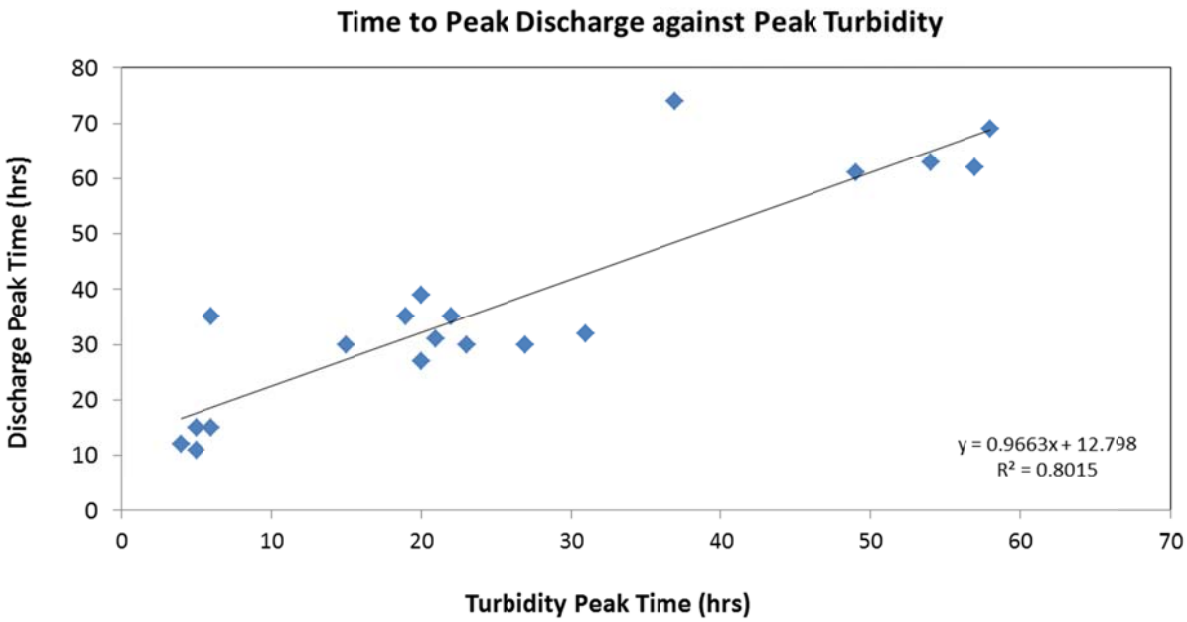

Figure 18: Discharge versus turbidity time to peak using USGS South Pass Road data.

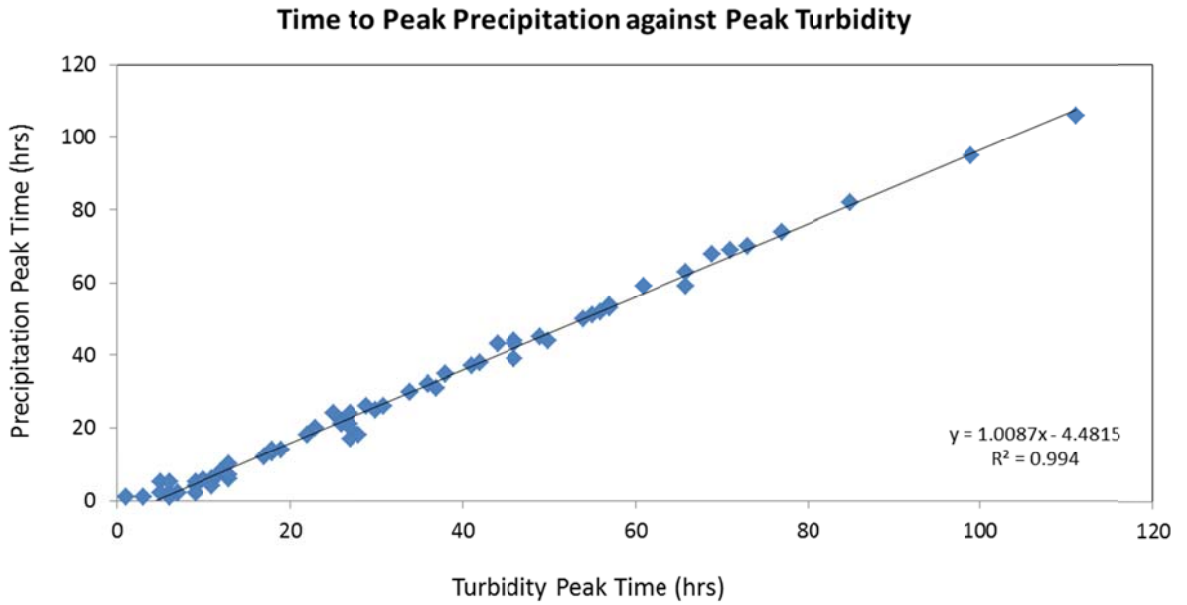

Figure 19: Precipitation versus turbidity time to peak using USGS South Pass Road data respectively.

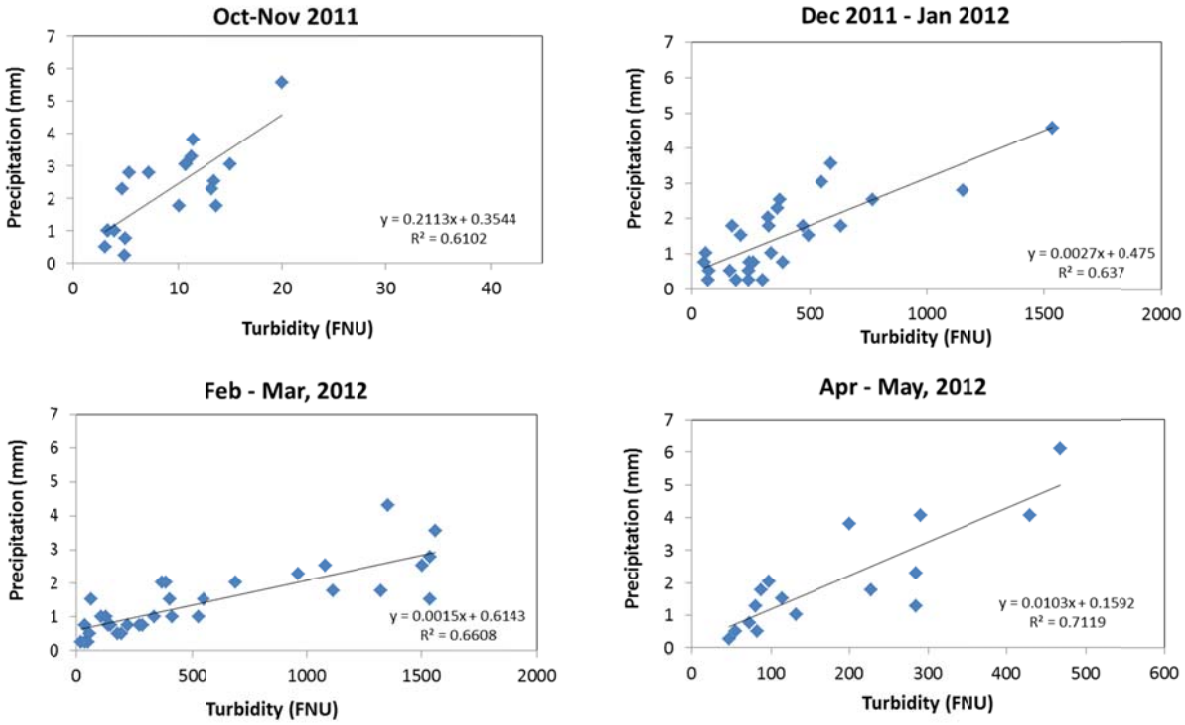

Figure 20: December 2011 to May 2012 precipitation and turbidity magnitudes plotted against each other. Precipitation from the Lawrence Station and turbidity from the USGS South Pass Road gauge.

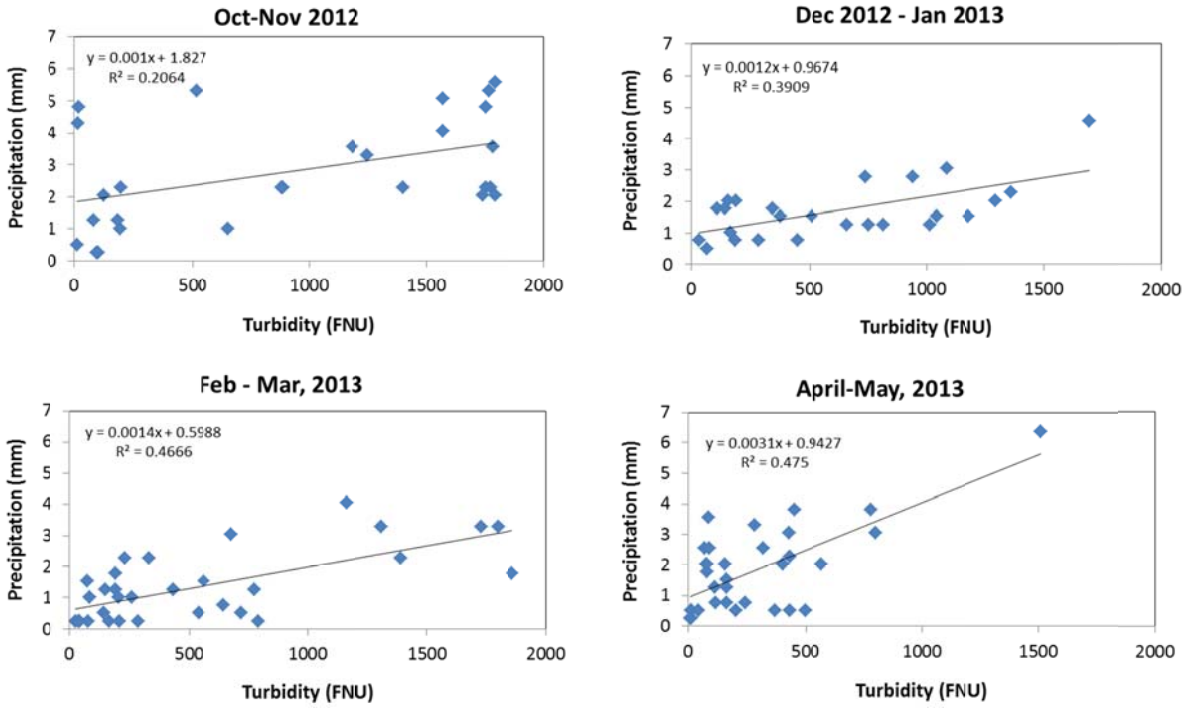

Figure 21: October 2012 to May 2013 precipitation and turbidity magnitudes plotted against each other. Precipitation from the Lawrence Station and turbidity from the USGS South Pass Road gauge.

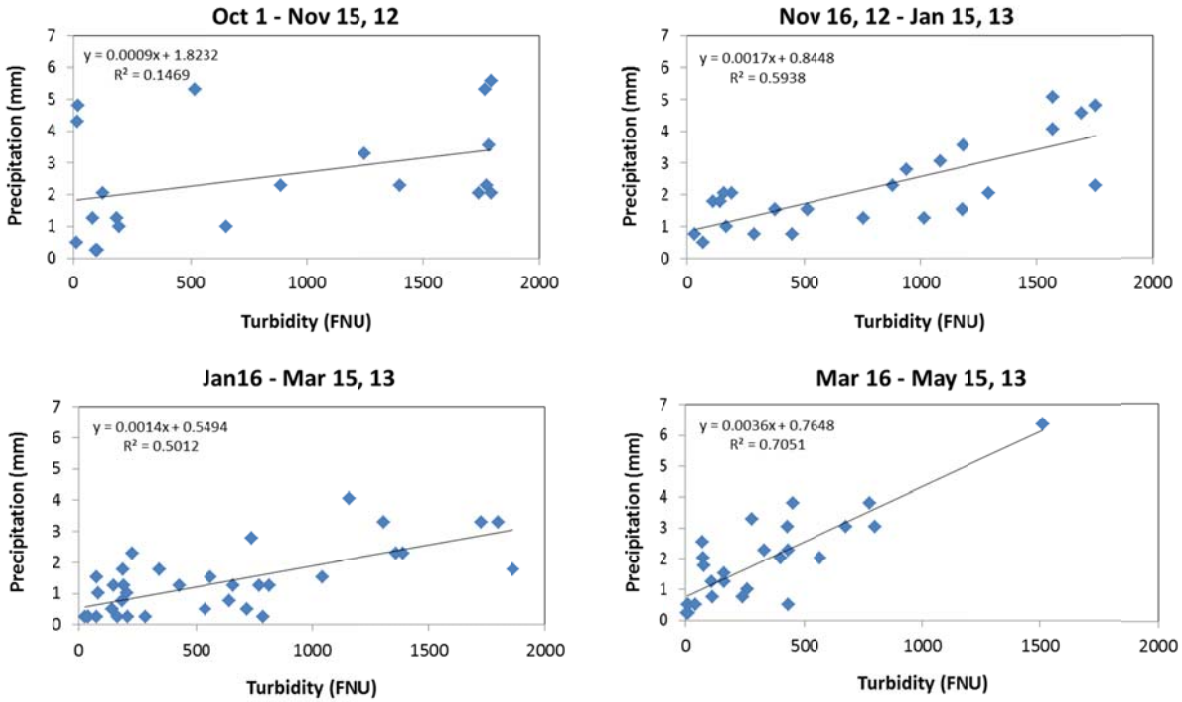

Figure 22: Shifted October 2012 to May 2013 precipitation and turbidity magnitudes plotted against each other. Precipitation from the Lawrence Station and turbidity from the USGS South Pass Road gauge.

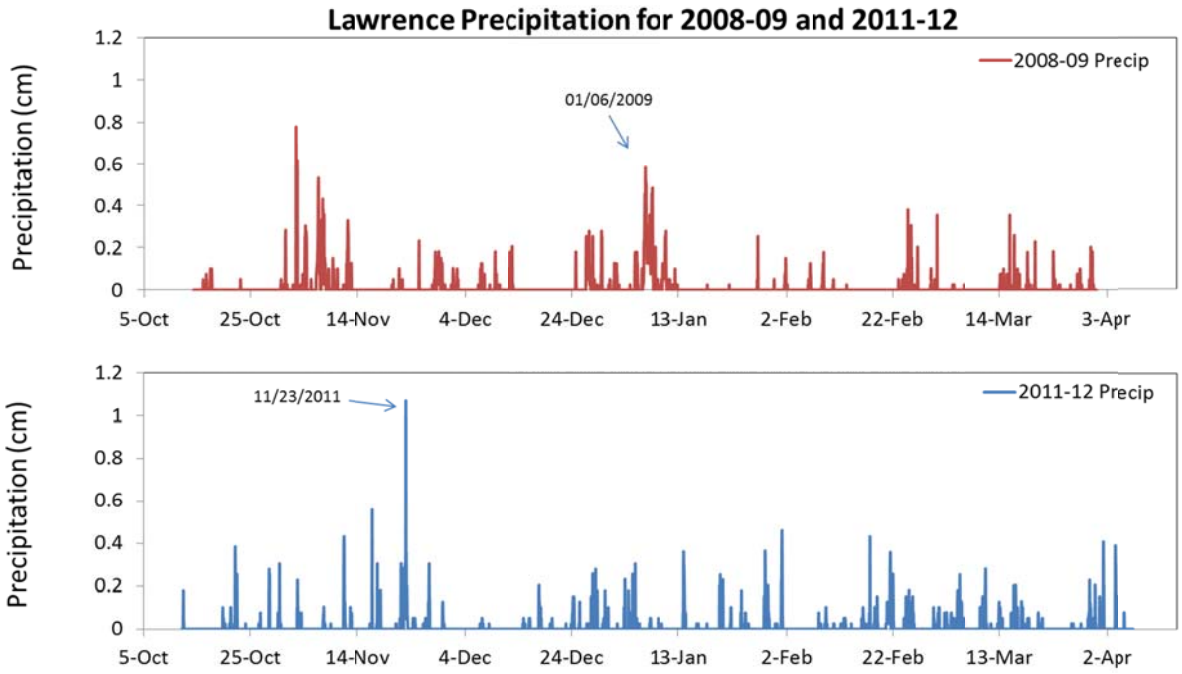

Figure 23: Comparison of 2008-09 and 2011-12 precipitation from the Lawrence Station.

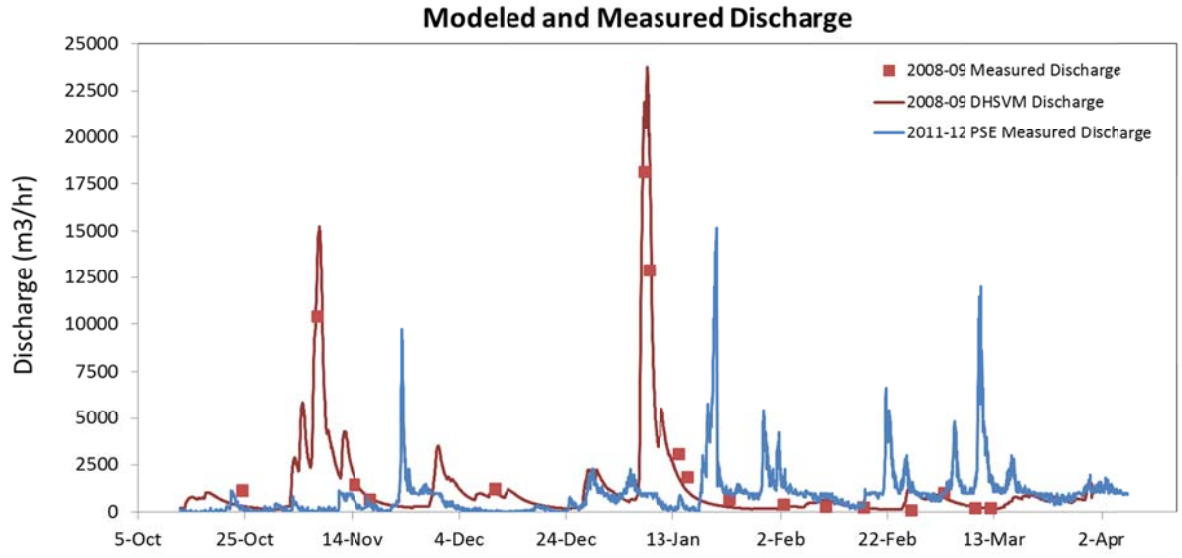

Figure 24: My 2008-09 measured and DHSVM discharge plotted with PSE's 2011-12 measured discharge to compare the two seasons.

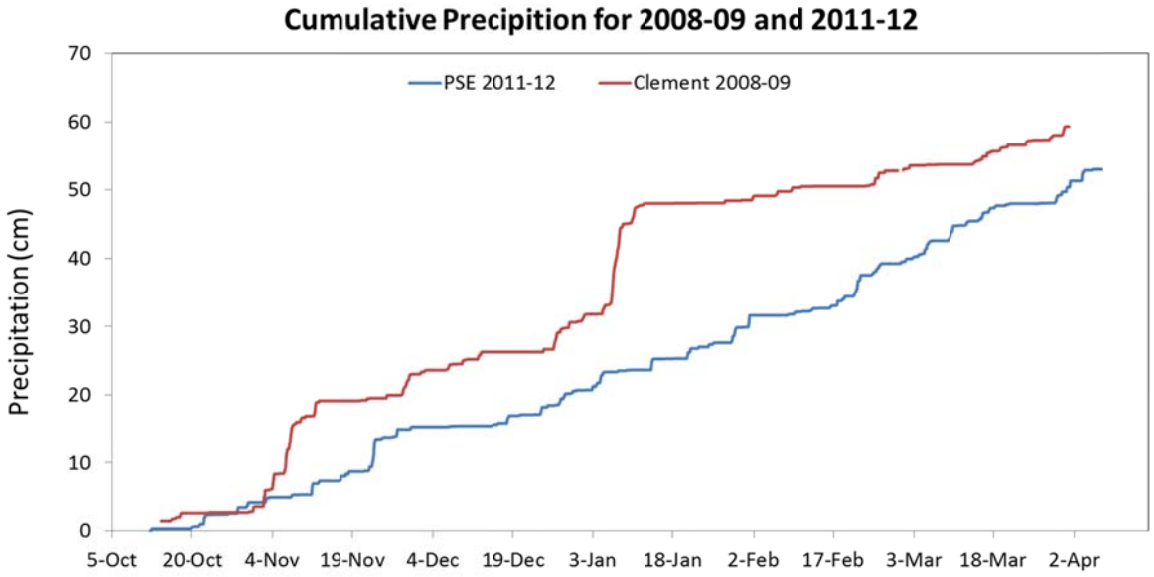

Figure 25: Cumulative precipitation from Lawrence station comparing my 2008-09 season and PSE's 2011-12 season.

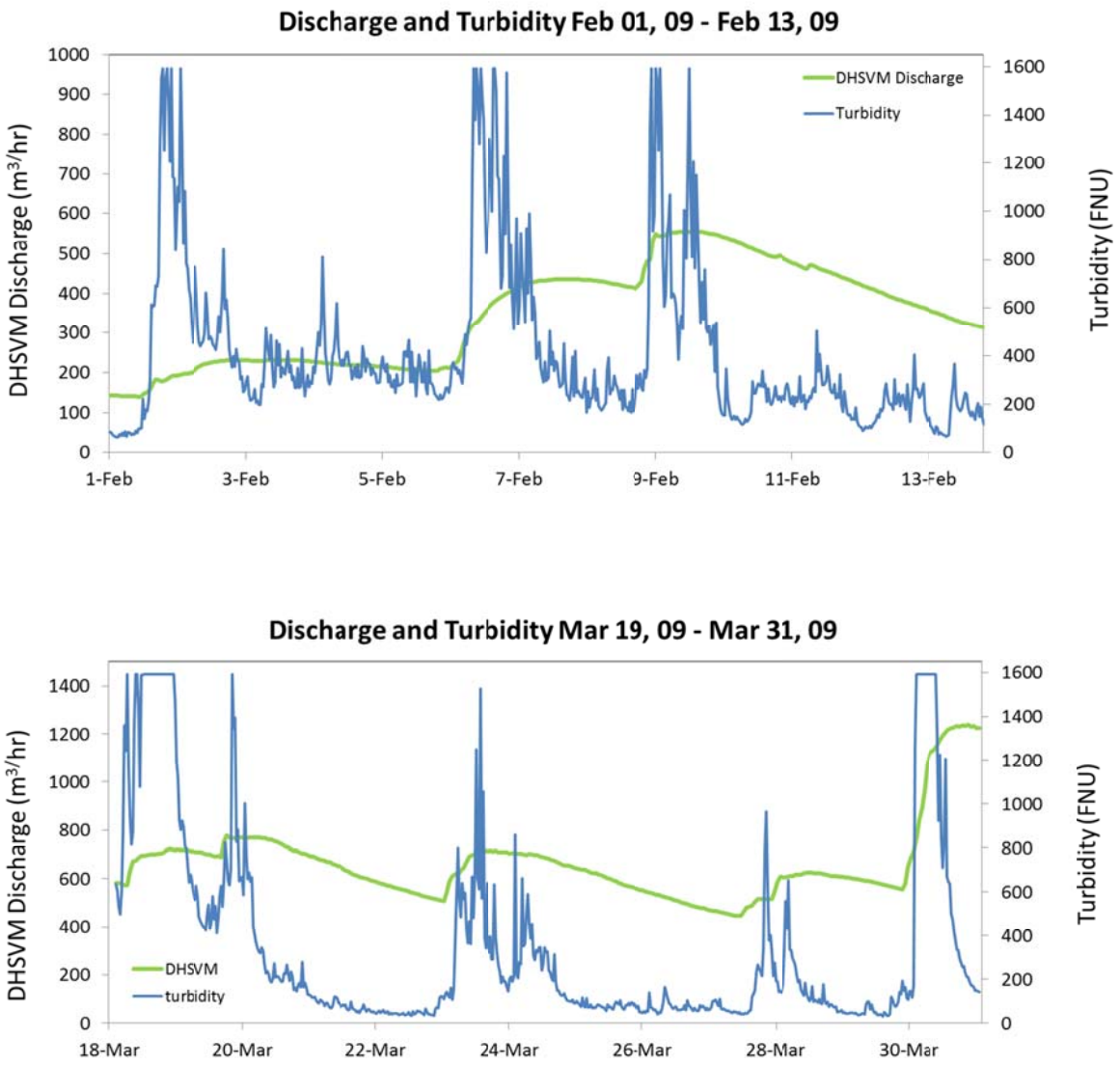

Figure 26: My Swift Creek DHSVM discharge and turbidity data from the Goodwin Road Bridge, 2008-09, demonstrating the effectiveness of the turbidity sensor and methods, and the agreement between discharge changes and turbidity.

Figure 27: Turbidity sensor in high water. Photo of my Goodwin Road Bridge gauging station taken January 7, 2009 during the largest discharge event of the season. View is to the east, streamflow is toward the bottom left.

Figure 28: Turbidity sensor close to stream bed. Photo of my turbidity sensor housing at the Goodwin Road Bridge taken February 1, 2009. View is to the north, streamflow is to the left. The stream bank is growing laterally toward the sensor from both sides. The southern bank (bottom of the photo) eventually engulfed the housing as I found on my Feb 17th visit. See Figure 29.

Figure 29: Turbidity sensor fouling. Photo of my turbidity sensor housing at the Goodwin Road Bridge taken February 17, 2009. View is to the south, streamflow is to the right. The southern bank (top of the photo) experienced rapid growth over the previous two weeks, extending out to the sensor housing. Compare to Figure 28.

Figure 30: Manual treamflow gauging on Swift Creek. Photo taken at Goodwin Road Bridge on November 7, 2008 prior to the full installation of the stream gauge. Submerged debris were striking our legs and feet. View is to the north and flow is to the left.

Figure 31: Thick ice formations on Swift Creek. Photo taken on December 27, 2008 of the sensor housing from the northwest footing of the bridge. View is to the south to show the thickness of ice and snow that covered much of the stream.

Figure 32: North Fork and South Fork turbidity difference. The clear North Fork (bottom left) is in stark contrast to the turbid South Fork of Swift Creek. Streamflow is to the right.

Figure 33: Washed out portions of the Great Western Creek in January 2009. Photos were taken by Mr. Crompton. The creek is labeled on Figure 3. He donated these photos at a chance meeting at the Goodwin Road Bridge.

APPENDIX A: TTS Stream Gauge Setup

To run the TTS methods using the FTS HDL1 Data Logger with the ISCO 3700 you will need the SDI-12 FTS SDI-Sampler Interface, the interface cable, and a 12 volt battery. To download data from the HDL1 you will need a Keyspan USB-Serial adapter (Specifically recommended by either FTS), and a true male/female DB9 serial cable. All the cables, batteries, and adapters have been purchased and are in the care of Dr. Scott Linneman.

The following setup options must be selected to configure the ISCO water sampler to be triggered by the FTS turbidity data logger. Explanations of the functions of these settings can be found in the ISCO Manual.

On the ISCO control panel step through the following menu options:

Enter Program

- Program = FLOW
- Sample = every 1 pulse
- Multiplex Samples = NO
- Sample Volume = 500 ml
- Calibrate Sample Volume = NO
- Enter Start Time = NO

Configuration

- Set Time = Sync with FTS
- Bottles = PORTABLE, 24, 500 ml
- Suction Line = 3/8, VINYL, 25 ft
- Liquid Detector –
    - ENABLE, 1 Rinse Cycle
    - Enter Head Manually = NO
    - Retry = 0 times
- Programming Mode = BASIC
- Calibrate Sensor = ENABLE
- Start Time Delay = 1 minute

- Enable Pin –
    - Master/Slave mode = NO
    - Sample Upon Disable = NO
    - Sample Upon Enable = NO
    - Reset Sample Interval = NO
    - Inhibit Countdown = NO
- Event Mark = PULSE At beginning of PURGE
- Purge Counts = 150 Pre-sample, 922 Post-sample
- Tubing Life - Reset Pump Counter = NO
- Program Lock = DISABLE
- Sampler ID = Nothing
- Run Diagnostics (Tests Functionality of moving parts and firmware)
    - Re-initiate test = NO

The last step of this setup is to "Run Diagnostics" which will take a couple of minutes after which you will have the option to re-initiate tests. Select NO or it will run the process over again.

Please NOTE: When you leave this in the field, you must push the "START SAMPLING" button on the ISCO Control Panel or it will sit there and do nothing until you come back. As you can imagine, this is very disappointing.

APPENDIX B: Sediment Yield Estimate Procedures

These are the steps I used for calculating the sediment yield.

1. Create TSS-Discharge correlation using measured TSS (mg/L) and DHSVM discharge (cfs) for the same time that the TSS sample was taken. The cfs was converted from the original DHSVM output of m^3/time step, in my case hours.
2. Apply TSS-Discharge equation to the DHSVM discharge (cfs) hourly data to create a continuous TSS (mg/L) hourly data set.
3. Take the original DHSVM output (m^3/hr) and convert to L/hr.
4. Multiply the new TSS data series (mg/L) with the new discharge (L/hr) to get Hourly Yield (mg).
5. Convert mg to kg by dividing mg/1,000,000
6. Sum the hourly yield to get the Total Yield (kg).
7. Convert to Volume (yd^3). Vol (yd^3) = kg*2.20462lbs/kg*cf/80lbs*0.03704yd^3/cf

I could have accomplished the same thing without using L/hr by multiplying the cfs by 3600 sec/hr and coverting cf to L.

I also accomplished the same thing by using a TSS-Discharge correlation using L/hr instead of cfs. See the tab called 'Straight LHr'

These are the steps PSE used for calculating the sediment yield.

1. Average the Modeled TSS (mg/L) to hourly data ('original process'!Col P). See the tab titled 'Hourly Formatting'
2. Average the discharge derived from stage data (cfs) to hourly ('original process'!Col N). See the tab titled 'Hourly Formatting'
3. Calculate the total volume of water and sediment passing the sensor per hour ('original process'!Col Q) by multiplying the average discharge in an hour by 3600 sec/hr.
4. Calculate hourly yield ('original process'!Col R) by multiplying the TSS (mg/L) by volume per hour (Col Q) and 28.317L/cf. Convert to kg by dividing this product by 1,000,000 mg/kg
5. Sum the hourly yield to get the Total Yield (kg) ('original process'!$R$4743).
6. Convert Total Yield to Total Volume (Yd3) ('original process'!$R$4744).

I reprocessed PSE data using the above process. I followed their spreadsheet as closely as possible. One change I made was to convert cfs to L/Hr and multiplying that straight to the Modeled TSS (mg/L) to get the hourly yield. See Column U and the totals are in cells U4743 and U4744.

This differs from PSE's spreadsheet. PSE left the volume per timestep in cubic feet and the timestep was not always constant. They include the conversion from cf to L in the solids per timestep equation.

The tab titled 'Turbidity-TSS 09' is where I determined Total Yield using my Turbidity-TSS Correlation.

The tab titled 'My dat, Paul's Trail' is where I took my DHSVM discharge (cfs) and applied Paul's equations, first Discharge-Turbidity and second Turbidity-TSS. I wanted to see what I'd get. In 'original process'!Col M I do the opposite and apply my Discharge-TSS equation to Paul's discharge (cfs).

APPENDIX C: Set up Procedures for GIS Inputs

The GIS inputs for DSHVM in this study were processed using ESRI ArcMap. The base GIS input is the DEM. The DEM sets the projection and grid spacing for all the other GIS inputs and is used to define the boundary of the watershed and the stream network using several processes in ArcMap. Other inputs required by DHSVM are land Cover, soil texture, soil thickness, and a streamflow network. In this manuscript, the level of detail is intended for those familiar with ArcMap software.

Defining the Watershed Boundary with the DEM

The DEM is the basis for all the spatial inputs and I obtained a USGS 10m DEM for this study from the following University of Washington website: http://duff.geology.washington.edu/data/raster/tenmeter/

I downloaded the necessary quadrangles, unzipped and converted to raster files for use in ArcMap. The converted raster files were used to create a DEM mosaic. At this point the watershed boundary must be defined using following the steps listed next.

Fill sinks

Determine flow direction of water for each grid cell

Determine flow accumulation

Determine the pour point of the basin. I selected the stream gauge location.

The watershed boundary was created using the hydrology/models toolbar that uses the flow direction and accumulation rasters to determine what grid cells contribute water toward or into the stream that will eventually end up at the selected pour point.

The raster created by this process has the shape of the watershed and is used to create a polygon of the same shape. This polygon is frequently used as a mask to clip the other GIS data to the watershed boundary.

Land cover

The Landcover data was downloaded from http://www.csc.noaa.gov/crs/lca/pacificcoast.html

These data are already in an ArcMap format and therefore do not need any file type conversion but they do need to be placed into the correct coordinate system and resampled to have the same resolution as the DEM. Once this is accomplished, use the watershed mask to clip the landcover data to the watershed boundary. Now re-classify the vegetation categories used by NOAA into categories understood by DHSVM.

Soil Texture

The soil texture data was downloaded from the STATSGO soil dataset http://www.soilinfo.psu.edu/etc/statsgolist.cgi?statename=Washington

These data come in the Interchange File format .e00 and must be converted to raster files with the same projection and grid spacing as the DEM. This will require more steps than before because the e00 is first converted into a polygon and then into a raster. There are three e00 files to download to have a complete soil texture map for DHSVM. The layer and comp files are tables that have specific information on each soil type.

Convert the e00 into coverages

Change the coordinate system

Clip the polygon to the watershed

Join layer and comp files by MUID using the join and relate function

Convert polygon to raster

Change the symbology to display all values of the category TEXTURE 1

I had to add a section in my soil texture map for the landslide. I have to re-figure out how I did that. This sucks but it was that difficult. I'm sure I wrote it down, but where?

Soil Depth and Stream Network

Soil Depth and stream network

The soil depth and stream network are created at the same time using an AML that is available from the DHSVM website. This AML is run in ARC info workstation. In the command to run the AML you will specify the area contributing to a stream segment and the min/max soil depths in order to achieve soil depths and stream segment density that are appropriate for the watershed.